

A novel multi-objective PSO for electrical distribution system planning incorporating distributed generation

S. Ganguly · N.C. Sahoo · D. Das

Received: 14 August 2009 / Accepted: 30 April 2010 / Published online: 18 May 2010
© Springer-Verlag 2010

Abstract This paper presents a novel particle swarm optimization (PSO) based multi-objective planning approach for electrical distribution systems incorporating distributed generation (DG). The proposed strategy can be used for planning of both radial and meshed networks incorporating DG. The DG plays an important role in the distribution system planning due to its increasing use motivated by reduction of power loss, voltage profile improvement, meeting future load demand, and optimizing the use of non-conventional energy sources etc. The overall approach consists of two multi-objective planning stages. In the first stage, a contingency-based multi-objective planning is used to optimize the number of feeders and their routes, and the number and location of the sectionalizing switches. In the second stage, the optimum siting and sizing of the DG units is determined for the networks obtained in the first stage by another multi-objective optimization. The multiple objectives of the first planning stage are: (i) minimization of the total installation and operational cost, and (ii) maximization of network reliability. The reliability of the distribution network is evaluated by a reliability index, i.e., contingency-load-loss index (CLLI), defined as the ratio of the average non-delivered load due to failure of all branches, taken one at a time, to the total load. The objectives for the second stage optimization are the DG penetration level and the total power loss. A set of non-dominated solutions/networks is obtained by simultaneous minimization of the conflicting objectives (at each stage) using the Pareto-optimality principle based trade-off analysis. A novel multi-objective PSO (MOPSO) is proposed for solving these optimization problems using a technique for selection and assignment of leaders/guides for efficient search of the non-dominated solutions. The selection of the leaders makes use of the available non-dominated and dominated solutions. The proposed planning algorithm is tested for the static and expansion planning of typical 100-node and 21-node distribution systems, respectively. The computer simulation results are critically






S. Ganguly · N.C. Sahoo (✉) · D. Das
Department of Electrical Engineering, Indian Institute of Technology, Kharagpur 721302, India
e-mail: ncsahoo@ee.iitkgp.ernet.in

evaluated. The performance of the algorithm is compared with that of the popular Strength Pareto Evolutionary Algorithm-2 (SPEA2)-based PSO and few other existing MOPSO techniques by means of statistical tests to highlight the efficacy of the proposed scheme.

Keywords Power distribution system planning · Multi-objective optimization · Particle swarm optimization · Pareto-optimality · Distributed generation

List of principal symbols

C_{IO}	total installation and operational cost (\$)
C^{Ib} (C^R)	branch installation (conductor replacement) cost per unit length (\$/km)
C^{Mb}	annual branch maintenance cost (\$/km/year)
l_j	length of branch j in km
C^V	total cost of energy losses (\$/year)
t_a	total planning time (in years)
C^{Is} (C^{Ms})	substation Installation (maintenance) cost (\$)
C^{Isw}	installation cost of a sectionalizing switch (\$)
C^{Ibkr} (C^{IT})	installation cost of a circuit breaker (tie line) (\$)
N_b (N_e)	number of new (existing) branches in the network
N_s (N_{Sw})	number of substations (sectionalizing switches)
N_F (N_{loop})	number of feeders (loops)
y_j	a binary variable (=1 if conductors are to be replaced; =0 otherwise)
D_F	discount factor ($D_F = \frac{1}{(1+u)^{ta}}$; u is interest rate)
CLLI	contingency-load-loss index
NDL_{avg}	average non-delivered load
NDL_i	non-delivered load due to fault in branch i
$L_{total}(\vartheta)$	total load (load loss factor)
P_{total}^l (P_i^l)	total real power loss (real power loss in branch i)
$\Psi(R_i)$	DG penetration index (active power rating of the i -th DG)
N_{DG} (n_i^{DG})	number (site/node of the i -th DG unit) of DG units
$iter$	superscript denoting iteration number
$PV_{i\theta}^{iter}$ ($X_{i\theta}^{iter}$)	velocity (position) of i -th particle in the θ -th dimension in iteration $iter$
ϕ_1 (ϕ_2)	learning constants (1.5–2.5)
r_1 (r_2)	random number $\in [0, 1]$
$pbest_{i\theta}^{iter}$	best position of the i -th particle in the θ -th dimension in iteration $iter$
$nbest_{i\theta}^{iter}$	neighborhood best of the i -th particle in the θ -th dimension in iteration $iter$
w	inertia weight
N_{loop}	number of loops
Z_i^s (Z_i^e)	start (end) zone for tie branch of i -th loop
n_{F_i} ($N_{Sw}^{F_i}$)	number of load nodes (switches) in feeder F_i
n	number of load nodes served by the substation
\times	circuit breaker

	feeder branch
	tie-line with switch (normally open)
	sectionalizing switch in feeder branch (normally closed)
	substation
	node/load point
Bold numeral	branch conductor size
<i>Italic numeral</i>	node number

1 Introduction

During the last decade, deregulation has resulted in significant restructuring of power systems. This motivates power system planners to design efficient, reliable, and cost effective power networks. Thus there is a great need for efficient distribution system planning algorithms. State-of-the-art reviews of the existing distribution system planning models can be found in [1, 2]. Distribution system planning is an optimization process to obtain a number of design variables such as: (i) size and location of the substation, (ii) number of feeders and their routes, (iii) number and locations of the sectionalizing switches, and (iv) radial or meshed network structure. The determination of the optimal value of these variables is done by meeting multiple objectives such as: (i) minimization of the installation cost of new facilities (i.e., substations and feeders), (ii) minimization of the operational (maintenance and lost energy) cost, and (iii) maximization of the system reliability. These objectives must also meet several network constraints, for example, substation and feeder capacity, and maximum allowable node voltage deviation.

Mostly, the distribution networks are designed to be radial for operational convenience and lower protection cost [1–15]. Total installation and operational cost is minimized by optimizing the number of feeders, their routes, and the number and locations of the sectionalizing switches. Network reliability is traditionally maximized by minimizing the (cost of) non-delivered energy due to faults [3–15]. The non-delivered energy is generally computed using the average failure rates and the repair durations of the feeder branches. However, it is very difficult to estimate the actual failure rates of the branches as the faults occur due to various unpredictable non-technical reasons, such as short circuit due to contact of small tree branches, animals etc. [16]. Moreover, the fault repair duration varies with the location and severity of the fault. Thus, this reliability evaluation may suffer from considerable inaccuracy.

Presently, the distribution networks are slowly changing from passive to active due to adoption of distributed generation (DG) [17, 18]. In the deregulated power market, the DG can be used as a valuable option for improvement of service quality, carbon emission reduction, supply for future load demand, less land requirement, and the utilization of the non-conventional local resources such as wind (and solar) energy. In all the previous works, the site and size of the DG units are optimized for radial networks only [19–30]. However, the meshed networks have the potential to accommodate much more generation than the radial networks [17, 18].

Considering the above issues in distribution system planning, the two-fold contributions of this work are: (i) planning of both radial and meshed networks using a

novel reliability index, and (ii) incorporation of the DG units into both meshed and radial networks at the planning stage. A contingency based reliability assessment indicator, named as *contingency-load-loss index* (CLLI) as proposed in [41], is used. The CLLI is defined as the ratio of the average non-delivered load due to failure of all branches, taken one at a time, to the total load. This index can distinguish reliability levels of different network structures (i.e., radial/meshed, single/multi-feeder networks). In the first stage, the CLLI and the total network cost are the two conflicting objectives used for determination of possible network structures as well as the number and locations of the sectionalizing switches. In the second stage, the optimum site and size for the DG units for the networks obtained in the first stage are determined by another multi-objective optimization, i.e., minimization of DG penetration level and power loss.

The simultaneous optimization of the multiple objectives can be done in many ways, for example, aggregating approach [3–8], Pareto-dominance based approach [9–15], lexicographic ordering [35, 42], and non-Pareto based approach [42]. Most of the multi-objective optimization algorithms are based on the Pareto-dominance principle [31, 35, 42] which is used to yield a set of non-dominated solutions. In this work, the Pareto-based approach is also used.

The distribution system planning problem is a nonlinear, non-convex, non-differentiable, constrained optimization problem with integer and continuous decision variables. Normally, the numerical optimization tools such as nonlinear programming (NLP) [3, 4], dynamic programming (DP) [5, 6], and benders' decomposition [9] have been used. There are some disadvantages with these analytical approaches, i.e., curse of dimensionality, non-differentiability, discontinuous objective space etc. In this regard, the heuristics-based algorithms have distinct advantages, i.e., they can handle nonlinear, non-convex problems, and do not require any gradient information. Some of the heuristics-based algorithms proposed for this planning problem are: genetic algorithm (GA) [7, 10–13], network flow programming [8], Tabu search [14], artificial immune system (AIS) [15] etc. Another powerful heuristics-based algorithm, successfully used in many complex problems, is the particle swarm optimization (PSO) [32, 33]. The advantages of the PSO over the other evolutionary algorithms are easy implementation, effective memory use, less number of function evaluations, and an efficient maintenance of diversity [34]. In this work, a novel multi-objective PSO (MOPSO) is proposed for the simultaneous optimization of the objective functions. The proposed method uses a novel technique for selection and assignment of leaders for the MOPSO population members. In the PSO formulation, a novel cost-biased encoding/decoding scheme is used to obtain the network structures; it prevents the creation of infeasible networks thereby overcoming a drawback of the direct encoding [11–15]. The proposed planning algorithm is tested on typical 100-node and 21-node distribution systems. The performance is assessed and compared with that of another powerful multi-objective optimization algorithm, i.e., Strength Pareto Evolutionary Algorithm-2 (SPEA2)-based PSO¹ [35, 36], and a number of other existing PSO-based multi-objective optimization algorithms by statistical tests.

¹As SPEA2 is a multi-objective optimization algorithm, the SPEA2-based PSO is also a kind of MOPSO.

The paper is organized as follows. The multi-objective distribution system planning problem is formulated in Sect. 2. The planning algorithm using the proposed MOPSO is presented in Sect. 3. Section 4 provides the simulation results and the performance assessment. Section 5 concludes the paper. The Appendix includes the basics of the short-circuit calculation for distribution systems, the SPEA2-based PSO, the statistical Mann-Whitney rank sum test, and the load demands of 21- and 100-node distribution systems.

2 Multi-objective distribution system planning problem

The distribution system planning used in this work is split into two stages keeping several factors in mind for which DG integration may not be possible, such as unavailability of appropriate locations, fuels, non-conventional local resources, i.e., wind, solar energy etc. In these circumstances, the first stage planning is only required to optimize the network structure.

2.1 Planning Stage I: determination of network structure

This planning stage deals with the construction of economical and reliable network. The first objective deals with the minimization of *total installation and operational cost*, while the second objective is the minimization of the CLLI. The objective function 1 consists of the installation cost of new facilities (substations, feeder and sectionalizing switches), the maintenance costs of the substations and feeders, and the cost of the energy losses. The objective function 2 measures network reliability with the CLLI. These two objective functions are mathematically expressed as:

Objective function 1:

$$\begin{aligned}
 C_{IO} = & \sum_{j=1}^{N_b} (C^{I_b} l_j + C^{M_b} l_j t_a + C^V P_j^l \vartheta D_F) \\
 & + \sum_{j=1}^{N_e} (C^{R_l} l_j y_j + C^{M_b} l_j t_a + C^V P_j^l \vartheta D_F) + \sum_{k=1}^{N_s} (C_k^{I_s} + C_k^{M_s} t_a) \\
 & + \sum_{m=1}^{N_{Sw}+N_{loop}} C_m^{I_{Sw}} + \sum_{k=1}^{N_F} C_k^{I_{bkr}} \tag{1}
 \end{aligned}$$

Objective function 2:

$$CLLI = \frac{NDL_{avg}}{L_{total}} = \frac{(\sum_{i=1}^{N_b} NDL_i) / N_b}{L_{total}} \tag{2}$$

The computation of the CLLI is illustrated with four possible network structures as follows:

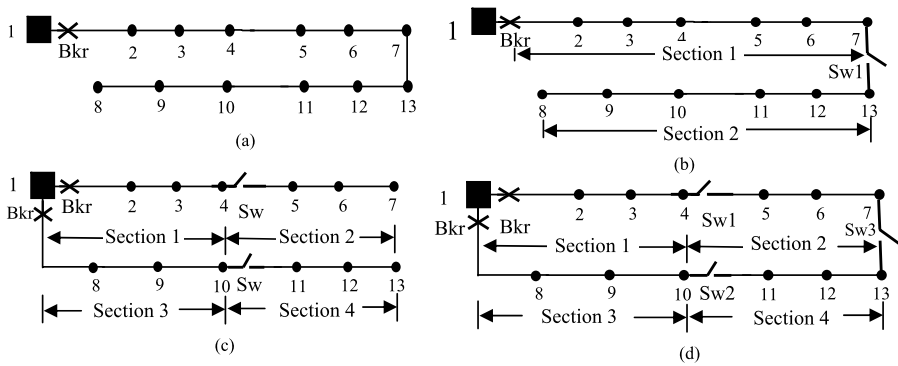


Fig. 1 Different types of distribution networks (a) single feeder radial network without any sectionalizing switch and (b) single feeder radial network with a sectionalizing switch, (c) two feeder radial network with two sectionalizing switches, and (d) meshed network with three sectionalizing switches

- single feeder radial networks without (Fig. 1(a)) and with (Fig. 1(b)) sectionalizing switch,
- two feeder radial network (Fig. 1(c)) with two sectionalizing switches,
- meshed network (Fig. 1(d)) with three sectionalizing switches.

Node 1 is the substation and every other node has 100 kW load (assumed). In Fig. 1(a), for a fault in any branch, the circuit breaker will isolate all the nodes from the supply. Thus, the total non-delivered load for a branch fault will be 1200 kW. Since any branch fault results in the same total non-delivered load, the average non-delivered load for all the branch faults, taken one at a time, is: $(1200 \times 12)/12 = 1200$ kW. Thus, the CLLI for this network is 1. This is the maximum possible value of CLLI; hence this is the least reliable network from the non-delivered load point of view. In Fig. 1(b) with one sectionalizing switch (normally closed) between the nodes 7–13, the network has two sections, i.e., Sects. 1 and 2. For a fault in any branch of Sect. 2, the switch can be opened to maintain the supply to Sect. 1 and it causes a non-delivered load of 600 kW. But, a fault in Sect. 1 results in a total non-delivered load of 1200 kW. As each section has six branches, the average non-delivered load is: $(6 \times 1200 + 6 \times 600)/12 = 900$ kW and the CLLI for this network is $900/1200 = 0.75$; thus this network is more reliable than that of Fig. 1(a). For Fig. 1(c), the CLLI is $\{(2 \times 3 \times 300 + 2 \times 3 \times 600)/12\}/1200 = 0.375$ and this network is more reliable than the single feeder radial networks. For Fig. 1(d), the CLLI is 0.23; thus this network is the most reliable amongst all.

The conductor types, substation sizes, and the circuit breaker types are chosen from pre-defined sets. The breaker types are decided based on the short circuit capacity of the networks (discussed briefly in the Appendix). The simultaneous optimization of the two objective functions in this planning problem is performed as they conflict with each other due to the following factors:

- *Network structure:* A meshed network is more reliable but costlier than a radial network due to more number of branches and costly breakers/switchgears for higher short circuit level.

- *Number of feeders*: An increase in the number of feeders improves network reliability at the expense of higher installation cost due to additional circuit breakers.
- *Sectionalizing switch*: It improves the CLLI; but its cost increases the objective function 1.

2.2 Planning Stage II: siting and sizing of DG in the network

The benefits of the DG are [23–30]: reduction of power loss, voltage profile improvement, and utilization of the non-conventional local resources. Also, the DG may lessen the impact of future load growth. Hence many utilities are integrating the DG units into the distribution networks. This requires additional installation and operational cost. Moreover, the short circuit level of the network increases due to the presence of the DG and it makes the breakers and switchgears more costly. In this planning stage, the DG is included in the distribution networks obtained from the previous planning stage; the locations and sizes of the DG units are determined by another multi-objective optimization. The aim is to assess the benefits of DG penetration in terms of power loss and voltage profile. The objective functions are: (i) power loss with the DG and (ii) DG penetration index (defined as the ratio of the total DG capacity to the total load). The corresponding mathematical expressions are:

$$P_{total}^l = \sum_{i=1}^{N_b} P_i^l \quad (3)$$

$$\Psi = \left(\sum_{i=1}^{N_{DG}} R_i \right) / L_{total} \quad (4)$$

The power loss reduces with increasing DG penetration. Thus, it needs simultaneous minimization. The networks obtained in Stage I are tested with different DG penetration levels. This step helps a utility in choosing a network (from the set of non-dominated solutions) if it has future plans for DG integration. The induction and synchronous generator based DG units are used in this study.

2.3 Pareto-optimality principle [31]

This principle states that for an m -objective optimization (say, minimization) problem, a solution x is said to dominate another solution y if

$$\forall i, \quad f_i(x) \leq f_i(y), \quad \text{and} \quad \exists j, \quad \text{such that} \quad f_j(x) < f_j(y) \quad (5)$$

where $f_i |_{i=1, \dots, m}$ are the objective functions. This principle is used to find a set of trade-off solutions, i.e., non-dominated solutions, constituting a Pareto frontier where all the solutions are equally important, i.e., none is inferior to the other. Unlike a single objective case, the multi-objective optimization relies on a set of solutions instead of a single solution.

3 Proposed multi-objective PSO for distribution system planning

This section gives details of the proposed MOPSO and the multi-objective distribution system planning algorithm based on it for both the planning stages.

3.1 Particle swarm optimization: an overview

Particle Swarm Optimization is a population based multi-point search technique [32] that mimics the social behavior of a flock of birds and a fish school etc. The search starts with a population of search points called particles. Each particle is encoded by a position vector (initially chosen at random) and the position is updated by using its velocity (initially chosen at random) in successive iterations. The velocity is updated using its own previous best position (*pbest*) and by following the best neighborhood particle's position (*nbest*). The position and velocity update equations are:

$$PV_{i\theta}^{iter+1} = PV_{i\theta}^{iter} + \phi_1 r_1 (pbest_{i\theta}^{iter} - X_{i\theta}^{iter}) + \phi_2 r_2 (nbest_{i\theta}^{iter} - X_{i\theta}^{iter}) \quad (6)$$

$$X_{i\theta}^{iter+1} = X_{i\theta}^{iter} + PV_{i\theta}^{iter+1} \quad (7)$$

The fitness of a particle is determined by the objective functions. The iterative PSO is performed till some termination criterion is attained, for example, maximum number of iterations or a desired fitness. Several modifications to this basic PSO have been reported [33, 34]. Among them, one is that of a linearly decreasing inertia weight for balanced local and global search [33]. A higher inertia constitutes a global search with emphasis on previous experience and a lower inertia promotes local search. In this PSO variant, the velocity is updated as:

$$PV_{i\theta}^{iter+1} = w PV_{i\theta}^{iter} + \phi_1 r_1 (pbest_{i\theta}^{iter} - X_{i\theta}^{iter}) + \phi_2 r_2 (nbest_{i\theta}^{iter} - X_{i\theta}^{iter}) \quad (8)$$

The performance of PSO depends on information exchange among the particles, which is influenced by neighborhood topology [34]. The global best (*gbest*) and local best (*lbest*) are two widely used neighborhood topologies.

3.2 Proposed multi-objective PSO

A state-of-the-art review of the PSO-based multi-objective optimization algorithms can be found in [35, 42]. The Pareto-based MOPSO approaches aim to obtain a set of well-spread and well-distributed non-dominated solutions called the Pareto-approximation frontier (closer to the Pareto-optimal frontier, generally not known *a priori*) using proper selection of leaders for each particle so as to reach closer towards the Pareto-optimal frontier and an elite preservation mechanism to store the non-dominated solutions. The selection of the leaders is done by assigning a fitness value to each particle based on its non-domination rank in the Pareto-dominance-based approaches [42]. However, there are some disadvantages (discussed later in this section) as the non-dominated solutions are only preferred to be the leaders. A novel MOPSO is proposed in this work in which some dominated solutions are also considered as leaders similar to some of the non-Pareto-based approaches [44]. In the

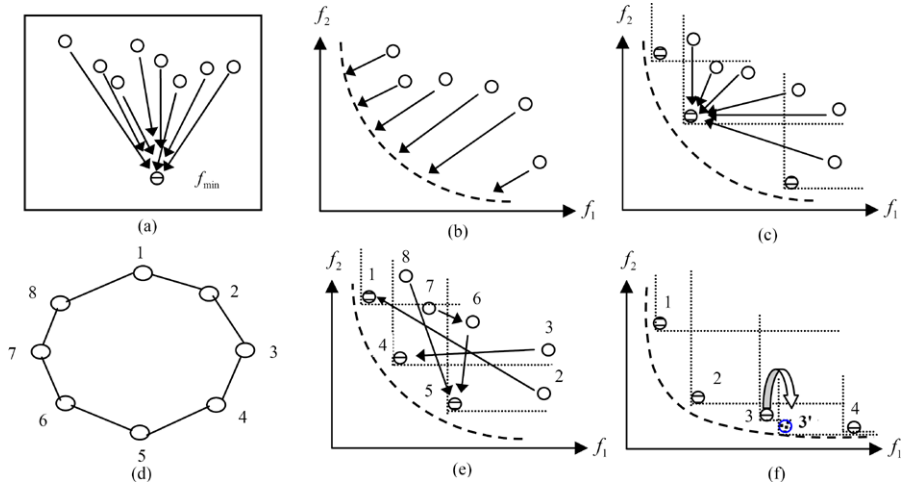


Fig. 2 Some typical search mechanisms of PSO: (a) unidirectional search by a population of particles for a single optimal position (mono-objective optimization), (b) multi-directional search for a set of Pareto-optimal solutions (multi-objective optimization), (c) a typical search process of SPEA2-based PSO with *gbest* topology, (d) information sharing among the particles in *lbest* topology, (e) a typical search process of SPEA2-based PSO with *lbest* topology, (f) a typical Pareto-optimal frontier with flat end regions

proposed method, the ideas behind the Pareto-dominance based approaches and the non-Pareto-based approaches are integrated to obtain better distribution of the Pareto-approximation solutions particularly for the problems having disconnected Pareto-approximation frontier. The performance of the proposed MOPSO is compared with those of some well-known MOPSO techniques.

Without any loss of generality, the proposed leader selection mechanism is explained for a bi-objective minimization problem. In PSO, the motion of a particle is guided by a leader chosen from the population. However, unlike a unidirectional search in mono-objective optimization (Fig. 2(a)), a multi-objective optimization needs a multi-directional search to reach closer to the Pareto-optimal frontier (Fig. 2(b)). In the SPEA2-based PSO with *gbest* topology, all particles follow the fittest particle (Fig. 2(c)) which may change over iterations; but in any iteration, the search is unidirectional. In *lbest* (ring) topology, a particle shares information with its immediate neighbors (Fig. 2(d)) and follows the fitter particle among its two immediate neighbors. Thus, in the SPEA2-based PSO with *lbest* topology, a multi-directional search can be obtained; but the search directions of the particles may not be towards the Pareto-optimal frontier specifically when a particle follows a dominated solution. Figure 2(e) shows such a case where the particle 7 follows the particle 6. Moreover, the search directions may frequently change over iterations preventing the convergence towards the Pareto-optimal frontier. Also, for problems with the two end regions of the Pareto-frontier being very much flat (Fig. 2(f)), a typical situation may arise as follows. As shown in Fig. 2(f), the difference between one objective function for two neighboring solutions (say, solutions 3 and 4) is very high compared to the difference between the other objective function in either end region of the Pareto-

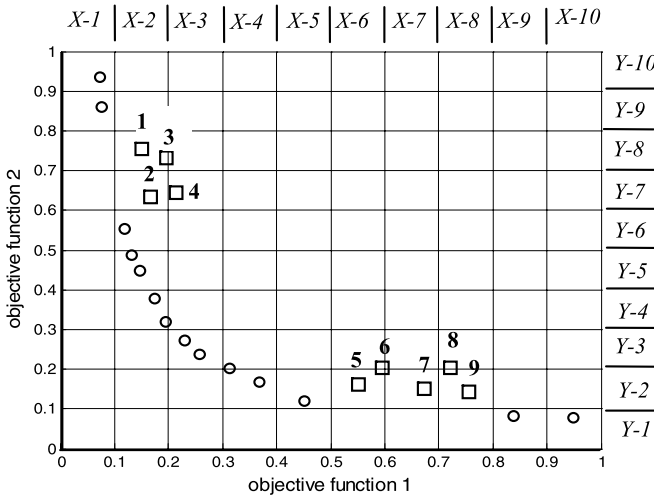


Fig. 3 A typical two-objective Pareto-approximation frontier along with non-dominated solutions and some dominated solutions in missing areas (where all solutions are dominated)

frontier. Thus, a little improvement of one objective of a solution (from solution 3 to solution 3') may cause domination of the other solution (solution 4). As soon as any solution gets dominated, the search direction is most likely diverted away from it. This prevents the chances of improvement of the solutions in those areas and those regions of the Pareto-approximation frontier may remain unexplored.

To overcome these difficulties, in the proposed MOPSO, the leaders are selected from the available non-dominated solutions and the fitter dominated solutions from those areas with no non-dominated solutions. The leader assignment is done heuristically to put more efforts to discover the non-dominated solutions in the unexplored areas. A typical two-objective Pareto-frontier is shown in Fig. 3 to illustrate this. It is seen that the non-dominated solutions (represented as circles) are missing in some areas; some dominated solutions in those areas are represented by squares. The computational steps for this in the proposed MOPSO are:

- Selection of a set of leaders uniformly distributed around the periphery of the Pareto-approximation frontier.
- Assignment of leader to each particle in the current population.

Selection of possible leaders The objective space is divided into a number of vertical and horizontal strips along the X- and Y-axis (say, X-1 to X-10 and Y-1 to Y-10) as shown in Fig. 3. The leaders are chosen by independent scanning of these strips. All the non-dominated solutions appearing in any strip are chosen as leaders and are named as the non-dominated leaders. If no non-dominated solution exists in any strip, then the dominated solution closest to the Pareto-approximation frontier is taken as a dominated leader. For example, in Fig. 3, there is no non-dominated solution in X-6, X-7, and X-8. Thus, the solutions 5, 7, and 9 are chosen as leaders for those strips, respectively. Similarly, the solutions 1 and 2 are considered as the dominated leaders for Y-8 and Y-7, respectively.

Begin

```

Initialize maximum iteration ( $Max\_iter$ ), population size ( $Pop\_size$ );
Perform PSO encoding to obtain initial population;
Decode all particles and calculate the objective functions;
Find out the initial non-dominated solutions;
Select the initial leaders (both dominated and non-dominated) and store them
in  $\{\Gamma\}$ ;
For  $i = 1, \dots, Max\_iter$ 
  For  $j = 1, \dots, Pop\_size$ 
    If  $j < (0.5 * Pop\_size)$ 
      Update velocity and position by following own best positions ( $pbest$ )
      and the position of its nearest non-dominated leader;
    Else
      Update velocity and position by following own best positions ( $pbest$ )
      and the position of its nearest dominated leader;
    Endif
  Endfor
  Decode the particle to calculate the objective functions;
Endfor
Delete all the old leaders (i.e.,  $\Gamma = \emptyset$ )
Find out the current non-dominated solutions;
Select new leaders and store them in  $\{\Gamma\}$ ;
Endfor

```

End**Fig. 4** Pseudocodes of the proposed MOPSO

Leader assignment A leader is heuristically assigned to each particle. To enforce the search in the unexplored areas, half of the members of the current population are assigned with their nearest dominated leaders and the rest are assigned with their nearest non-dominated leaders. The pseudocodes for the proposed MOPSO are given in Fig. 4.

The motivations behind the proposed approach may have some similarity with some heuristics-based approaches, for example, local competition in AIS or simultaneous use of the decision variable space and objective space. But, this method is not conceptually same as that of the local competition. The search in PSO is based on cooperation among the particles by information sharing, not on competition as in the GA or AIS. The proposed approach, in which a particle's leader is identified by distance measurement in the objective space only, is different from simultaneous use of the decision variable space and objective space.

3.3 Planning algorithm: Stage I

This subsection provides the details of the multi-objective planning algorithm based on the proposed MOPSO.

3.3.1 Proposed particle encoding/decoding scheme

The particle position vector is encoded using a combination of direct and indirect encoding schemes as shown in Fig. 5. A particle carries the following information:

- (i) *Node bias values* (ρ): Each node of the network is assigned a dimension in the position vector, named as *node bias values* (an indirect information), i.e., $\{\rho \in (-1.0, 1.0)\}$. A radial network structure is obtained by decoding this information (described later in the next page).
- (ii) *Number of feeders* (N_F): This component of the position vector gives direct information on the number of feeders in the network. It is kept below a specified maximum value.
- (iii) *Number of sectionalizing switches* (N_{Sw}): This provides direct information on the number of sectionalizing switches in the network. It is also kept below a specified maximum value.
- (iv) *Number and location (zone) of loops* (N_{loop}): This provides the information on number and locations of loops which are used to form the loops. The network area is divided into a number of zones as shown in Fig. 6(a). A node appears in a zone depending on its geographical location. The number of zones is problem specific. For a meshed network, firstly, a radial network is formed using the node bias values. Then, it is converted into a meshed network by creating N_{loop} number of loops. A loop is created by connecting any two nodes of the two selected zones, such as zones Z_1^s and Z_1^e (Fig. 6(a)). The number of loops is restricted between zero (i.e., radial structure) and a certain maximum value.

Figure 6(b) shows the particle decoding scheme. It consists of three steps as explained below.

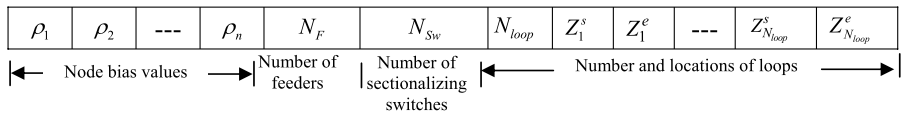


Fig. 5 Proposed particle encoding scheme

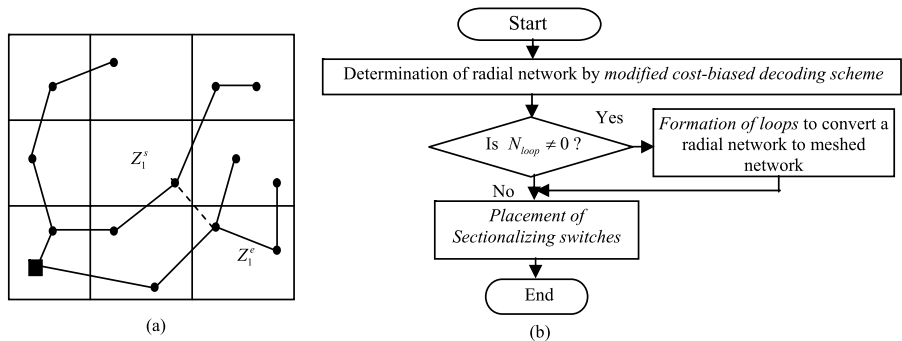


Fig. 6 (a) Loop creation mechanism, (b) flow chart of the proposed particle decoding scheme to obtain network structures

Begin

$\{Q\} \leftarrow$ substation node and nodes to be directly connected to the substation
 ($= N_F$) based upon distance calculations;

$\{R\} \leftarrow$ nodes to be connected with the network;

$\{\alpha_s\}, \{\alpha_e\} \leftarrow$ start and end nodes of the branches, respectively;

While ($R \neq \emptyset$)

For $i = 1, \dots, \text{size}(Q)$

For $j = 1, \dots, \text{size}(R)$

If $M(Q(i), R(j)) = 1$

$C(i, j) = \sigma(Q(i), R(j)) * \rho(j)$;

Endif

Endfor

Endfor

Find the *minimum element of C* and corresponding $Q(i)$ and $R(j)$

Update $\{\alpha_s\} \leftarrow \{\alpha_s, Q(i)\}$; Update $\{\alpha_e\} \leftarrow \{\alpha_e, R(j)\}$

Update $\{Q\} \leftarrow \{Q, R(j)\}$; Delete $\{R(j)\}$ from $\{R\}$

Endwhile

End

Fig. 7 Pseudocodes of the proposed particle decoding scheme to generate a radial network structure

Step 1: Creation of radial networks using a modified cost-biased decoding scheme.

In this decoding scheme, the nodes are selected and appended to the terminal node of a growing path on the basis of minimum value of the product of branch costs and node bias values [37]:

$$j = \arg \min \{\sigma(i, k) \rho_k\}, \quad \sigma(i, k) = \text{branch cost (nodes } i \text{ and } k) \quad (9)$$

To construct a radial network with main and lateral branches, this cost-biased decoding scheme is modified. In a distribution network, it is also preferred to connect a node with some neighboring nodes. This feature is incorporated by a binary connectivity matrix M ($n \times n$ matrix for an n -node system). If a connection between nodes i and j is allowed, $M(i, j) = 1$, else $M(i, j) = 0$. The maximum number of allowable connections for a node is problem specific. Figure 7 shows the pseudocodes of the decoding scheme to generate a radial network. The length of a branch is taken as its cost. Initially, the to-be-connected nodes are stored in an array $\{R\}$, and the substation and the other already connected nodes (if any) are stored in another array $\{Q\}$. Two more arrays (initially empty for new network) are used to store the start and end nodes of the branches. The number of nodes directly connected with a substation is restricted to the number of feeders (N_F) obtained from the particle and they are selected based on minimum distances from the substation. Those nodes are deleted from $\{R\}$ and added to $\{Q\}$; $\{\alpha_s\}, \{\alpha_e\}$ are updated accordingly.

Step 2: Formation of loops (for meshed network). In this step, the radial network is converted into a meshed network. The zones, in which the start and end nodes of a loop-forming branch are located, are obtained from the particle. From these two zones, any two randomly selected nodes are connected to form a loop.

Step 3: Placement of sectionalizing switches. Now, the sectionalizing switches are heuristically placed based on the number of switches obtained from the particle. The switch locations are determined as follows:

- The number of switches in an individual feeder (say feeder F_i) is determined as:

$$N_{Sw}^{F_i} = \text{round}\left(\frac{n_{F_i}}{n} N_{Sw}\right) \quad (10)$$

- The placement of the sectionalizing switches depends on two factors, i.e., (i) load demand, and (ii) number of branches in the feeder sections sectionalized by the sectionalizing switches. There are two strategies based on the *load demand at the nodes* and the *number of branches in the individual feeders*. The first strategy attempts to equalize the total load in different feeder sections. In the latter, the switches are conveniently (and uniformly) placed at equal distances for keeping equal number of branches in all the feeder sections as far as possible. For example, consider a 30-node feeder with a total load of 3000 kW and two sectionalizing switches are to be placed. In the first strategy, the switches are placed such that the loads in the three feeder sections are nearly 1000 kW each. In the second strategy, one switch can be placed in the branch just after the 10th node and the other in the branch just after the 20th node to have almost equal number of branches in the three feeder sections.

3.3.2 Conductor size selection

The conductor sizes are selected based on the tentative branch power flows to keep the branch flows below the respective rated capacities. All the branches of a network are firstly assigned lower conductor sizes and a load flow is performed to get the branch power flows. Then, the conductor sizes with immediate higher ratings than the respective branch flows are assigned.

3.3.3 Constraint handling techniques

The constraints of this planning problem are handled as follows:

- Feeder branch capacity is satisfied by the conductor size selection algorithm.
- If the node voltage limit constraint is violated, the solution is penalized by a suitable penalty factor. The penalty factor, computed as the product of the absolute value of the maximum node voltage deviation from a specified nominal value and a very high integer number, is added to the objective function 1. The performance with the proposed penalty factor method is compared with those of two existing methods, i.e., the method-H and the method-K [48].

The pseudocodes of the complete planning algorithm (for Stage I) are shown in Fig. 8.

Begin

// η_{pop} = size of PSO population
 // η_{gen} = Maximum number of iterations
 Generate *initial population* for PSO randomly using the proposed *encoding scheme* (both position and velocity);
 Decode the *particles* to obtain the networks and calculate the objective functions;
 Find the *initial non-dominated solutions* and store them in *elite archive*;
 Find out initial set of leaders;
 iteration = 1;

While iteration \leq η_{gen}

For $i = 1, \dots, \eta_{pop}$

Assign a leader for particle i from the set of leaders;
 Update *velocity* and *position* of the particle using (7)–(8);
 Decode *particle* to get the network structure;
 Select *conductor sizes* using conductor size selection;
 Calculate the short circuit levels of the network to choose the breaker ratings;
 Calculate the *objective functions* (see (1)–(2));

Endfor

Find out the *non-dominated solutions* and update *elite archive*;
 Find out the new set of leaders;
 iteration = iteration + 1;

Endwhile

Elite archive contains optimal network structures along with branch conductor-sizes and the number and locations of the sectionalizing switches;

End

Fig. 8 Pseudocodes for the distribution system planning (Stage I) using the proposed MOPSO

Fig. 9 Particle encoding scheme for Stage II optimization

N_{DG}	n_i^{DG}	---	$n_{N_{DG}}^{DG}$	R_i	---	$R_{N_{DG}}$
Number of DG units		Locations of DG units (node number)		Ratings of DG units		

3.4 Planning algorithm: Stage II

The non-dominated solutions/networks obtained from the planning Stage I are further evaluated for placement of the DG units of different sizes at different locations. The optimization objective functions are computed using (3)–(4). The constraints are the same as before. The particles are encoded with the information on the number of DG units, their sites and ratings (Fig. 9). The number of DG units is restricted between one and a specified maximum value. The possible sites may be any node (except substation). The ratings of the DG units are restricted to some specified discrete values. The decoding of particle is simple (fractions are rounded to the nearest feasible integer numbers). The proposed MOPSO is used to update the velocity and position of the particles. The pseudocodes of the complete algorithm are shown in Fig. 10.

Begin

// β_{pop} = Size of PSO population

// β_{gen} = Maximum number of iterations

Generate *initial population* for DG locations randomly (both position and velocity) for the networks representing non-dominated solutions obtained from the previous multi-objective planning optimization;

Decode the *particles* and calculate the objective functions;

Store the initial *non-dominated solutions* in *elite archive*;

Find out the initial set of leaders;

iteration = 1;

While *iteration* \leq β_{gen}

For $i = 1, \dots, \beta_{pop}$

Assign a leader for particle i from the set of leaders;

Update *velocity* and *position* of the particle using (7)–(8);

Decode *particle* to get number, sites, and sizes of DG units;

Perform load flow and calculate *objective functions* using (4)–(5);

Endfor

Find out *non-dominated solutions* and update *elite archive*;

Find out the new set of leaders;

iteration = *iteration* + 1;

Endwhile

Elite archive contains optimal network structures that have sites and sizes of distributed generators.

End

Fig. 10 Pseudocodes for the distribution system planning (Stage II) using the proposed MOPSO

4 Simulation results and analysis

The proposed planning algorithm is evaluated via computer simulation studies on two typical distribution systems. The first problem is a static problem, i.e., planning of a completely new 100-node network [11]. The second one is an expansion planning problem of a 21-node distribution system [11] with four existing branches. Some features of these two systems are:

- Each system has one substation. The load demands are given in the [Appendix](#).
- The conductor and circuit breaker specifications are given Tables 1 and 2, respectively.
- The substation capacity for the 100-node system is chosen as 15 MVA serving a total load of 12.63 MVA. Its installation cost is \$3,000,000. The total load demand of the 21-node system is 3.9491 MVA with substation capacity of 8 MVA.
- The substation voltage, the minimum and maximum node voltage are taken as 1.05 p.u., 0.92 and 1.08 p.u., respectively.
- The installation cost of each sectionalizing switch is taken as \$20,000.
- The maximum number of feeders and loops (both) are specified to be 5.
- The maximum number of allowable connections for a node is chosen as 8.

Table 1 Specification of conductor sizes

Conductor type	Current rating (A)	Branch installation cost (\$/km)	Preventive maintenance cost (\$/km/year)	Corrective maintenance cost (\$/km/year)	Resistance (ohm/km)	Reactance (ohm/km)
1	150	10000	533.54	6.51	0.5762	0.5184
2	230	15000	533.54	6.51	0.4724	0.2875

Table 2 Circuit breaker Specification

Circuit breaker type	Short circuit current rating (kA)	Installation cost (\$)
1	25	40000
2	35	60000
3	50	80000

The PSO parameters are optimized based on the growth of the non-dominated solutions. The performance of the proposed MOPSO is assessed and compared with that of the SPEA2-based PSO and some other existing multi-objective PSO algorithms by statistical tests. The results of the two planning stages for the static planning of the 100-node system are presented first followed by the results of the 21-node system expansion planning. A performance comparison with an existing (evolutionary) planning algorithm is also provided.

4.1 Results of distribution system static planning: Stage I

In this section, the results of planning Stage I are presented along with the performance assessment of the proposed MOPSO.

4.1.1 Optimization of PSO parameters

An appropriate choice of the PSO parameters, i.e., population size (η_{pop}), maximum number of iterations (η_{gen}), maximum and minimum velocities of particles (PV_{max} , PV_{min}), learning constants (ϕ_1 , ϕ_2), maximum and minimum inertia weight (w_{max} , w_{min}), is very important. The optimized values of η_{pop} and η_{gen} are chosen as 80 and 200, respectively, as an exhaustive simulation study shows that the growth of non-dominated solutions saturates within 200 iterations with a population size of 80 and a population size higher than 80 has very little influence. The other parameters are optimized empirically on the basis of growth of the non-dominated solutions and the optimized values are given in Table 3. The penalty factor is chosen to be of the order of 10^7 . The number of strips per objective is chosen as 15.

4.1.2 Analysis of Pareto-approximation frontiers

The Pareto-approximation frontiers obtained with both types of sectionalizing switch placement strategies are shown in Fig. 11. The results illustrate that both Pareto-approximation frontiers are very close. Hence, any one strategy can be used. The

Table 3 Optimized PSO parameters

PSO parameters	Optimized values
η_{pop}	80
η_{gen}	200
PV_{max}, PV_{min}	0.5, -0.5
ϕ_1, ϕ_2	2, 1.5
w_{max}, w_{min}	0.9, 0.1

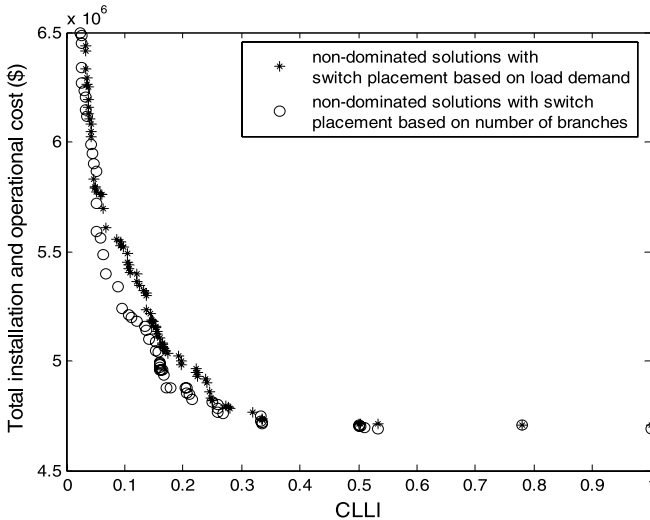


Fig. 11 Pareto-approximation frontiers obtained with switch placement based on the load demand and the number of branches in a feeder

Pareto-approximation frontiers obtained with the proposed MOPSO and SPEA2-based PSO with *gbest* and *lbest* topologies in a sample run are shown in Figs. 12–13. The Pareto-approximation frontier with the proposed MOPSO is classified according to the number of feeders, loops, and sectionalizing switches to distinguish the solutions on the basis of different structures (Figs. 14–16).

These results reveal the following salient features:

Remark 1 The Pareto-approximation frontier obtained with the proposed MOPSO is better than that obtained with the SPEA2-based PSO with both *gbest* and *lbest* topologies in terms of both convergence and diversity.

Remark 2 Many non-dominated solutions have the CLLI less than 0.3. The CLLI of a single feeder radial network without any sectionalizing switch is 1. A better CLLI (0.5–0.9) is obtained for double feeder radial network without sectionalizing switches. It is improved further if the radial network has multiple feeders and sectionalizing switches (Figs. 14–16). For meshed networks, the CLLI range is: 0.0–0.2. Obviously, the meshed networks have lower CLLI than the radial networks.

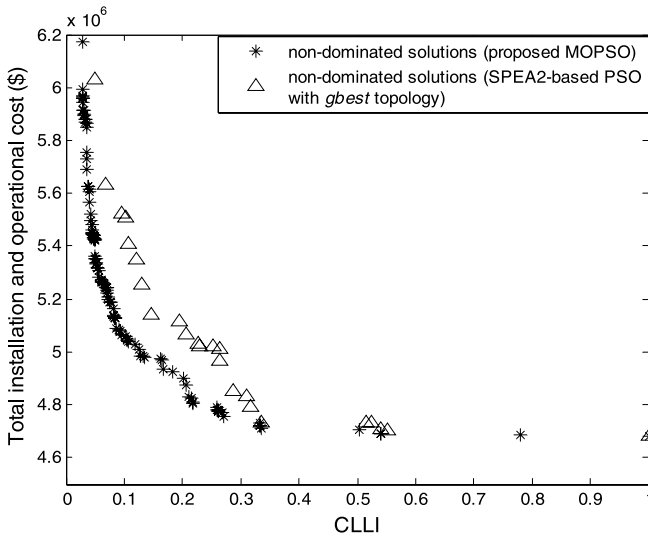


Fig. 12 Pareto-approximation frontiers obtained with proposed MOPSO and SPEA2-based PSO (*gbest* topology)

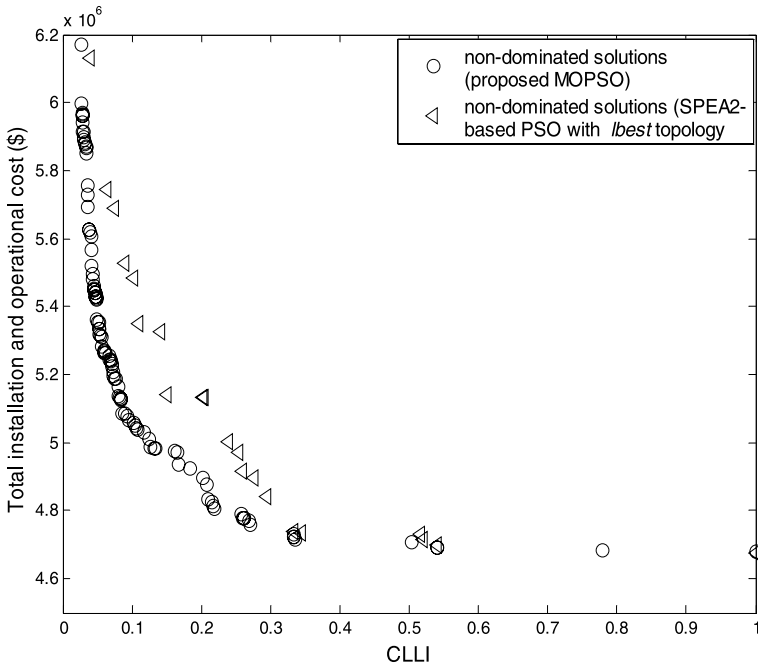


Fig. 13 Pareto-approximation frontiers obtained with proposed MOPSO and SPEA2-based PSO (*lbest* topology)

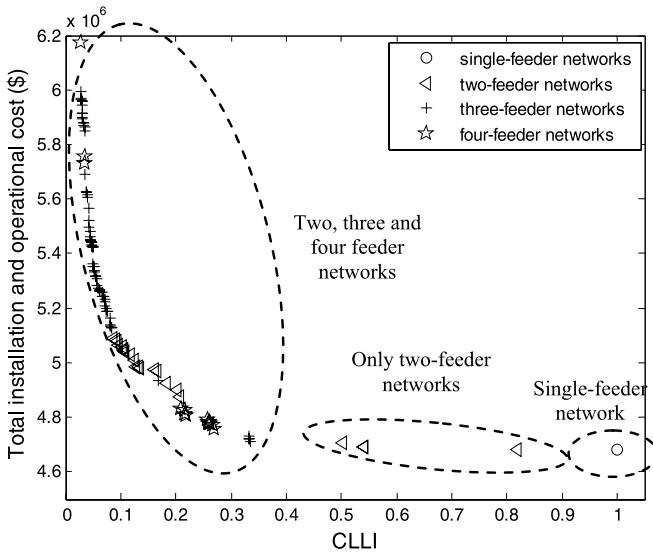


Fig. 14 Non-dominated solutions in the Pareto-approximation frontier (proposed MOPSO) classified according to number of feeders

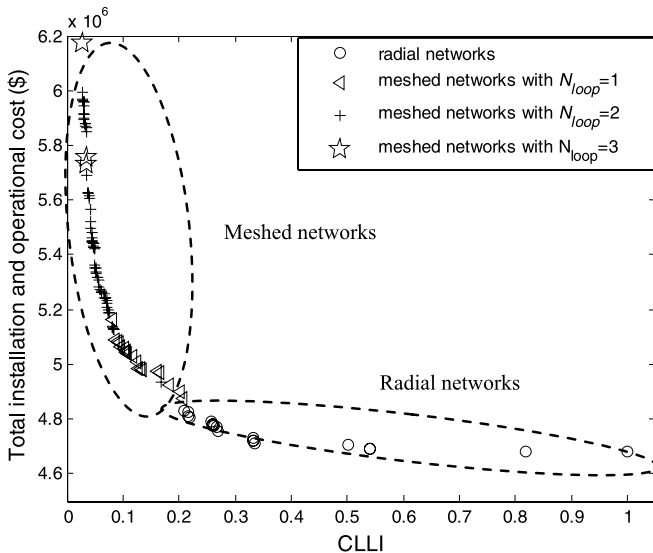


Fig. 15 Non-dominated solutions in the Pareto-approximation frontier (proposed MOPSO) classified according to number of loops

Remark 3 Figures 14–16 also show that the total installation and operational cost of the networks increases with higher number of feeders, loops, and the number of sectionalizing switches. Although both the maximum number of loops and feeders are specified to be 5, no solution is obtained with more than three loops and four feeders.

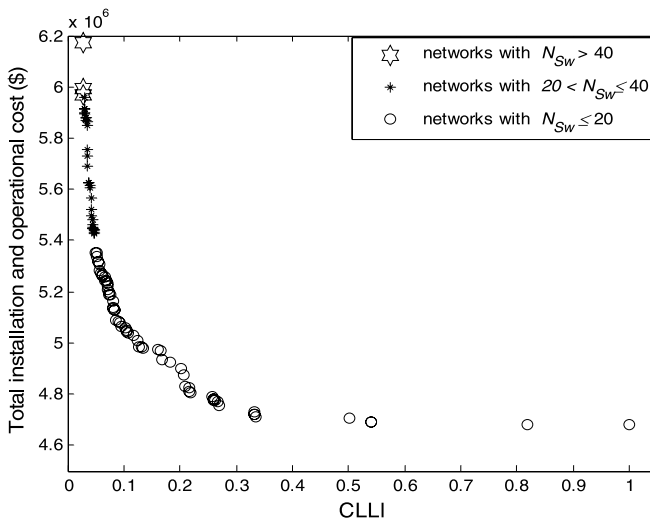


Fig. 16 Non-dominated solutions in the Pareto-approximation frontier (proposed MOPSO) classified according to number of sectionalizing switches

Also, the highest number of sectionalizing switches among all the non-dominated solutions is 41. This happens because the non-dominance test of the Pareto-optimality rejects a solution with higher feeders, loops, and sectionalizing switches if it fails to dominate the existing solutions.

Remark 4 The network is divided into 9 different zones (i.e., 3×3 grid) for loop creation. It is observed that less number of zones creates longer loop forming branches and higher number of zones has insignificant influence. It is seen that most of the meshed networks have inter-feeder loops than intra-feeder loops as an inter-feeder loop can improve the reliability more than an intra-feeder loop. The lowest power loss (130.67 kW) is obtained in a four-feeder radial network. The lowest power loss among all the meshed networks is 155.81 kW for of a three-feeder network with two loops. Normally the power loss of a meshed network is lower than that of a radial network with similar feeder routing. As meshed networks have longer loops (i.e., a large number of branches belong to a loop) to achieve good CLLI, the amount of power flowing through the root branches becomes higher. Thus, the power loss increases. Hence, power loss of a network depends not only on its structure (radial/meshed) but also on the feeder routing. It is also observed that the power loss is mostly influenced by the number of feeders and on the uniformity of load distribution among the feeders.

For the sake of illustration, two sample solution networks (most reliable and most economical) obtained with the proposed MOPSO are shown in Figs. 17–18, respectively and some typical features of these solutions are given in Table 4.

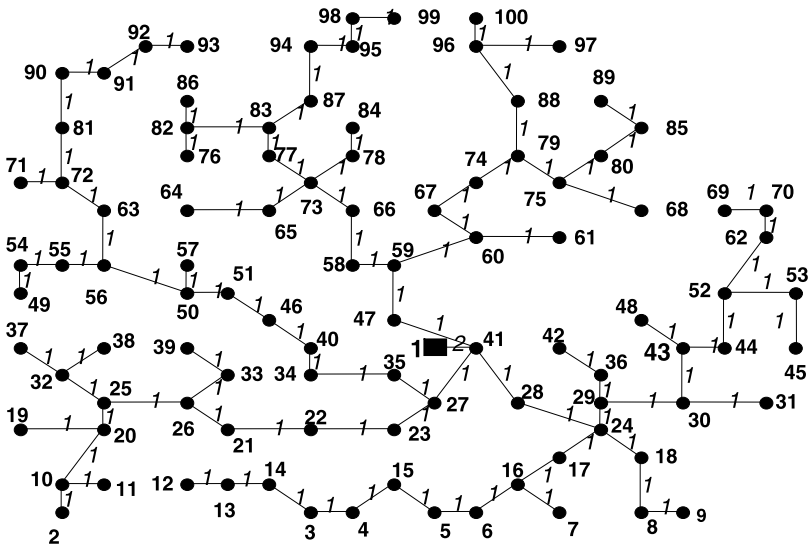


Fig. 17 Most economical network of Pareto-approximation frontier obtained with proposed MOPSO

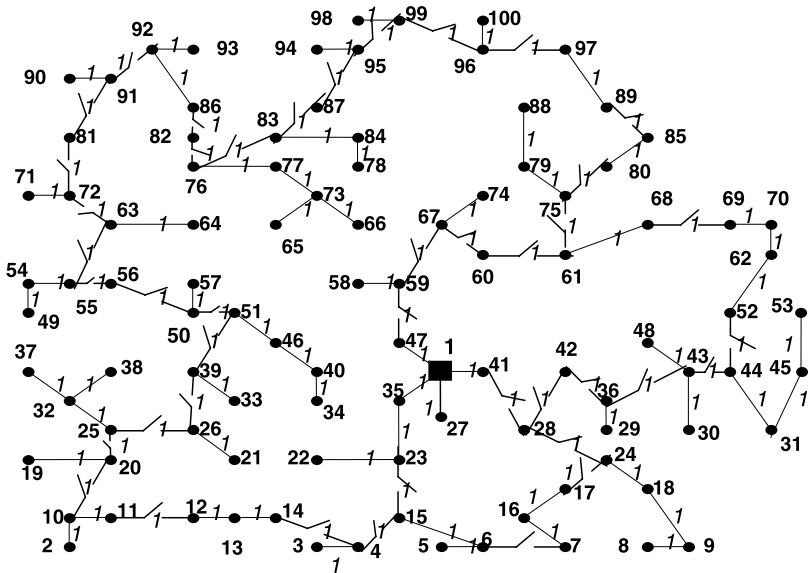


Fig. 18 Most reliable network of Pareto-approximation frontier obtained with proposed MOPSO. (Loop 1: nodes 1-35-23-15-6-7-16-17-24-28-41-1, Loop 2: nodes 1-41-28-42-36-43-44-52-62-70-69-68-61-60-67-59-47-1, Loop 3: nodes: 1-47-59-67-60-61-75-80-85-89-97-96-99-95-87-83-76-82-86-92-91-81-72-63-55-56-50-51-39-26-25-20-10-11-12-13-14-4-15-23-35-1

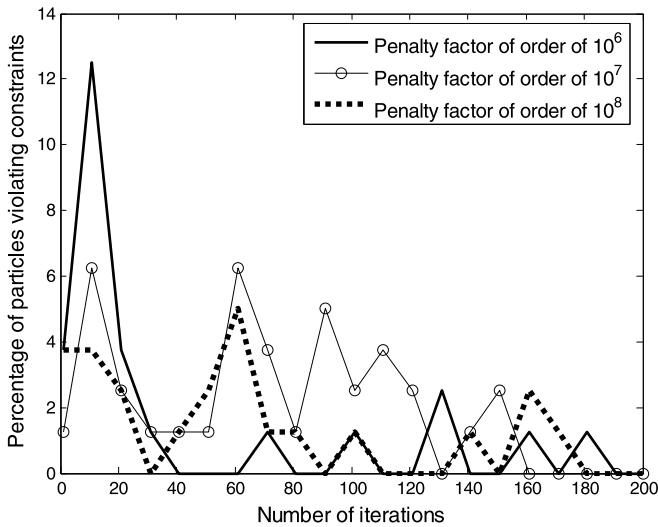


Fig. 19 Comparison of variations in percentage of particles (solutions) violating the constraints with different values of the penalty factors in the proposed method

Table 4 Some typical features of the most economical and most reliable networks

Solution	C_{IO} (\$)	CLLI	N_F	N_{loop}	N_{Sw}
Most economical	4.68×10^6	1	1	0	0
Most reliable	6.17×10^6	0.027	4	3	41

4.1.3 Impact of the penalty factor

A study is carried out to examine the impact of the penalty factor computed as the product of the absolute value of the maximum node voltage deviation from a nominal value and a very large positive integer number. In order to study the sensitivity of the choice of the large positive integer, three different values, i.e., of the order of 10^6 , 10^7 , and 10^8 , are chosen for investigations. The reason behind these specific choices is that the values of the objective function 1 of the solutions with this example system are of the order of 10^6 . The impact of these chosen values is evaluated by observing the changes in the percentage of particles violating the constraints with iterations (in typical sample runs), as shown in Fig. 19. The characteristics show frequent rises and falls with an overall decreasing trend, i.e., the number of constraint violations decreases with iterations on an average. The performance of the proposed penalty factor method (penalty factor of the order of 10^7) is also compared with those of two other existing methods, i.e., the method-H and the method-K [48]. The results over some typical sample runs, illustrated in Fig. 20, don't show any significant difference among the performances of the three methods. This highlights that the chosen penalty factor method performs quite well.

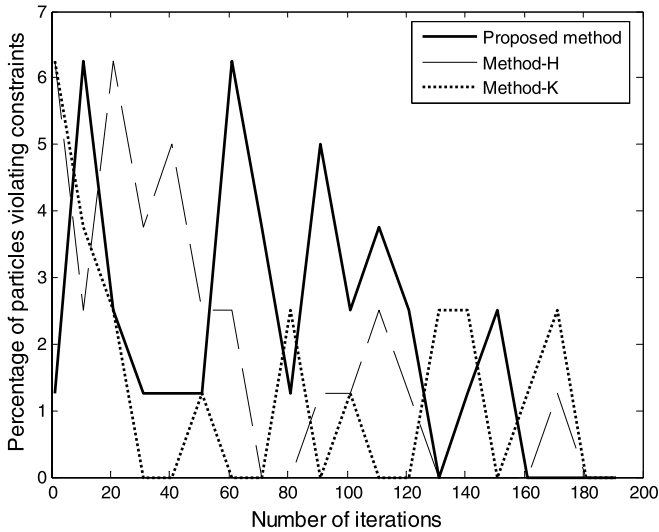


Fig. 20 Comparison of variations of percentage of particles (solutions) violating the constraints with the proposed method, the method-H, and the method-K

4.1.4 Performance assessment by statistical tests

The output of a single run of a stochastic multi-objective optimizer is an approximation set. However, no performance comparison is possible from the result of a single run. Thus, the statistical performances of the proposed MOPSO, the SPEA2-based PSO, and some other MOPSO variants are compared (over 25 runs) using the following performance measures.

A. Hypervolume indicator It is a unary indicator [38] used to measure the portion of objective space dominated by the Pareto-approximation set. A higher hypervolume indicator signifies a larger area dominated by the approximation set and thus it has better performance. Figure 21 shows the boxplots of the hypervolume indicator for different runs (with reference point $(7.5 \times 10^6, 1)$ in the objective space) of both the proposed MOPSO and the SPEA2-based PSO with *gbest* and *lbest* topologies. The growths of the cumulative hypervolume indicators for these three algorithms are shown in Fig. 22, which also clearly illustrates the superior performance of the proposed MOPSO.

B. Summary attainment surface plot As the solutions of an approximation set cannot be interpolated with a smooth curve, it is very difficult to visualize and assess the quality of different approximation sets of same or different optimizers. Thus, the best way to measure the performances of a Pareto-approximation set is to identify the goals that have been attained by this approximation set [38]. This can be obtained by a summary attainment surface plot. A summary attainment surface is a boundary comprising of all the tightest goals attained by a particular optimizer after a specified number of trial runs. The tightest goals after certain number of trial runs are the

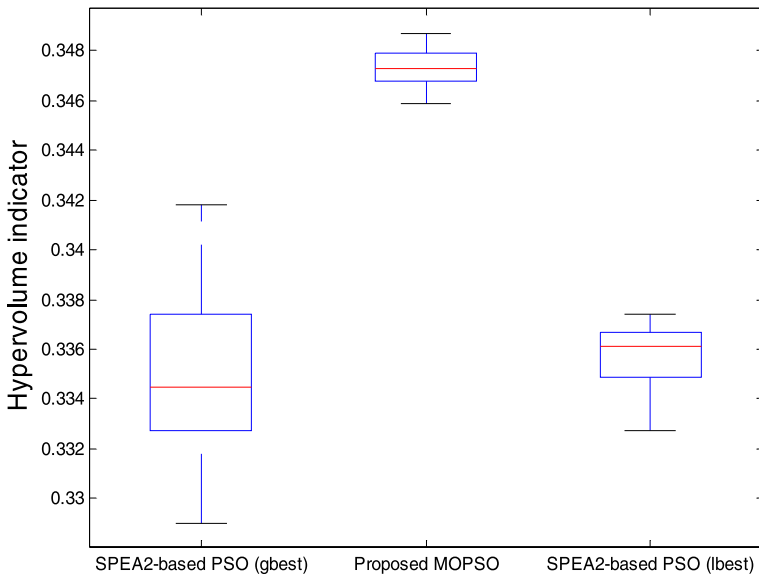


Fig. 21 Boxplots of hypervolume indicators with the SPEA2-based PSO (*gbest* and *lbest* topologies) and the proposed MOPSO

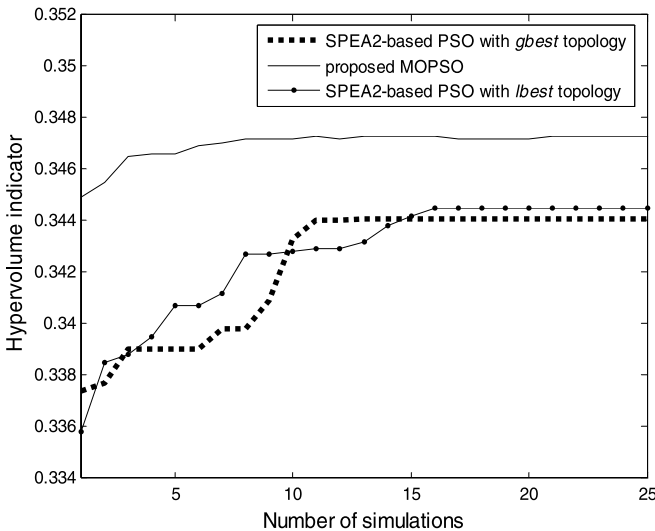


Fig. 22 Growth of cumulative hypervolume indicators of the SPEA2-based PSO (*gbest* and *lbest* topologies) and the proposed MOPSO obtained after different runs

resultant non-dominated solutions amongst all Pareto-approximation sets. The summary attainment surface plots after 25 trial runs (Fig. 23) show that the proposed MOPSO has superior performance over the SPEA2-based PSO (both *gbest* and *lbest* topologies).

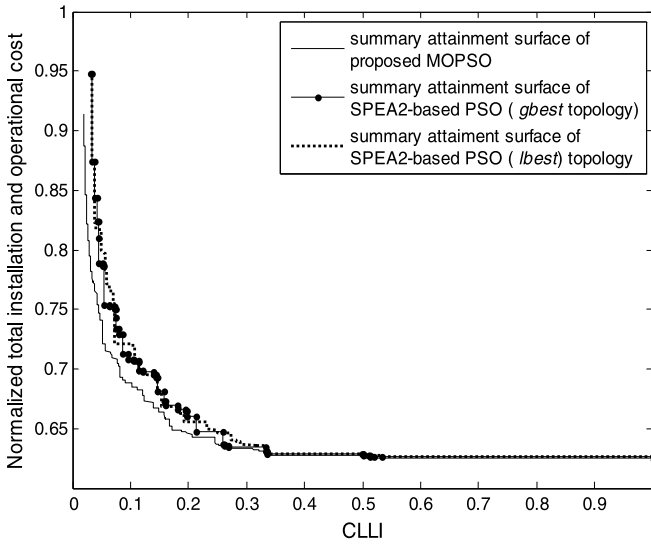


Fig. 23 Summary attainment surface plots of the SPEA2-based PSO (*gbest* and *lbest* topologies) and the proposed MOPSO

C. Mann-Whitney rank sum test The Mann-Whitney rank sum test is a non-parametric test to provide indications about any significant difference between two groups of observations. In this test, at first, all the data of the two groups are combined and a rank is assigned to all data of both the groups. Thereafter, a statistic U is assigned to both the groups. The null hypothesis is rejected if the minimum U between the two groups is less than or equal to the critical value. The calculation of the U statistic is given in the [Appendix](#). In this study, the hypervolume indicators obtained from 20 different runs with the proposed MOPSO and the SPEA2-based PSO (for both *gbest* and *lbest* topologies separately) are grouped. The minimum U value (= 49) is found to be less than the critical value (105) under 1% significance level for both *gbest* and *lbest* topologies. This illustrates that there is a significant difference between the performances of the proposed MOPSO and the SPEA2-based PSO.

D. Diversity indicator The diversity indicator (Δ) measures the diversity among the obtained η_{ndf} number of non-dominated solutions. It is defined as [31]:

$$\Delta = \frac{\sum_{i=1}^{\eta_{ndf}} |d_i - \bar{d}|}{\eta_{ndf} \bar{d}} \tag{11}$$

Ideally, the distance between any two nearest solutions (d_i) should be equal to the mean distance (\bar{d}) between any pairs of solutions. Thus, a lower value of this indicator indicates a better diversity. The distances between the extreme solutions of the Pareto-approximation frontiers and the Pareto-optimal frontiers are not considered as the Pareto-optimal frontier is unknown. The values of the diversity indicator with the proposed MOPSO, the SPEA2-based PSO using *gbest* topology, and the SPEA2-based PSO using ring (*lbest*) topology are obtained as 0.9699, 0.9863, and 0.9818,

Table 5 Comparison of hypervolume and diversity indicators obtained with the different MOPSO algorithms

Different MOPSO algorithms	Hypervolume indicator		Diversity indicator	
	mean	deviation	mean	deviation
Proposed MOPSO	0.3475	0.0018	0.9699	0.0184
SPEA2-MOPSO (<i>gbest</i> topology)	0.3345	0.0037	0.9863	0.0198
SPEA2-MOPSO (ring topology)	0.3361	0.0040	0.9818	0.0149
SPEA2-MOPSO (stochastic star topology)	0.3415	0.0012	0.9745	0.0244
NSMOPSO	0.3442	0.0013	0.9927	0.0149
VE-MOPSO	0.3348	0.00084	0.9777	0.0179
Sigma-MOPSO	0.3444	0.00098	0.9994	0.0196
CL-MOPSO	0.3322	0.001	0.9773	0.0187
Mocell-PSO	0.3411	0.005	0.9992	0.0191
Clonal-MOPSO	0.3406	0.00091	0.9927	0.0101

respectively. This highlights the improvements obtained with the proposed MOPSO over the SPEA2-based PSO.

A performance comparison of the proposed algorithm with some existing methods, i.e., the PSO stochastic star topology [45] applied in SPEA2, the Non-dominated Sorting MOPSO (NSMOPSO) [43], the Vector Evaluated MOPSO (VE-MOPSO) [42], the Sigma-MOPSO [43], the Comprehensive Learning MOPSO (CL-MOPSO) [43], the Multi-objective Cellular PSO (Mocell-PSO) [46], the Particle Clonal operator [47] applied in MOPSO, is carried out. The PSO parameters are taken to be same as given in Table 3. A summary of results over 25 runs is shown in Table 5. The reference point for measuring hypervolume indicator is $(7.5 \times 10^6, 1)$. The results show that the performance with the proposed MOPSO is improved in terms of both hypervolume and diversity indicators than all the algorithms studied here. The mean hypervolume indicators show that the convergence of the proposed MOPSO is comparable with those of the NSMOPSO and the Sigma-MOPSO. On the other hand, the mean diversity indicators show that the proposed MOPSO is capable of obtaining diversified solutions comparable to those in the SPEA2-MOPSO (stochastic star topology), the CL-MOPSO, and the VE-MOPSO. In terms standard deviations of hypervolume and diversity indicators, the performance of the proposed MOPSO may not be the best, but comparable with those algorithms. In conclusion, the overall results illustrate the improvement in performance with the proposed MOPSO over the existing methods studied here.

Finally, it is to be noted that this stage of planning can give various network structures from which a utility can choose one final network depending on its requirement.

4.1.5 Sensitivity test with different number of strips per objective

There is also an additional parameter in the proposed MOPSO, i.e., the number of strips per objective. A sensitivity test is required for performance assessment with different number of strips per objective. The sensitivity test results for this static

Table 6 Hypervolume and diversity indicators with different number of strips per each objective

Number of strips per each objective	Mean hypervolume indicator	Mean diversity indicator
5	0.3439	0.9945
10	0.3447	0.9823
15	0.3475	0.9718
20	0.3479	0.9721
25	0.3475	0.9714

Table 7 Optimized PSO parameters for Stage II planning

PSO parameters	Optimized values
β_{pop}	20
β_{gen}	200
PV_{max}, PV_{min}	0.5, -0.5
ϕ_1, ϕ_2	2, 1.5
w_{max}, w_{min}	0.9, 0.1

planning problem are summarized in Table 6. It shows that both the convergence and diversity improve with increasing number of strips per objective up to a certain point beyond which no significant improvement occurs. It can be observed that, for this problem, 15 strips per each objective happen to be a reasonably good choice (which has been used in all the studies). Obviously, the optimal number of strips per objective is a problem specific parameter.

4.2 Results of distribution system static planning: Stage II

In this planning stage, the impact of DG penetration is investigated. The networks considered for this stage of planning are the non-dominated solutions/networks obtained from the Stage I. For a comprehensive study, 20 solutions/networks are uniformly sampled from the Pareto-approximation set obtained in Stage I; the sampled networks are shown in Fig. 24 (in the objective space). Out of the 20 solutions, 7 solutions (solution numbers 14–20) have radial structures and 13 solutions have meshed structures (solution numbers 1–13). The number of strips per objective is taken to be 15. Some typical data used in this study are:

- Four different sizes for the DG units are considered. They are: 500 kW, 1000 kW, 1500 kW, and 2000 kW.
- The installation and operational costs of the DG units are taken as $\$5 \times 10^5$ per MVA and \$70 per MWh, respectively [29].
- The optimized PSO parameters used in this stage of planning are given in Table 7.

Three case studies are carried out with different types of DG units, i.e.,

- *Case A:* The DG units are synchronous generators with power factors of 0.8 lagging. They are operated in the voltage control mode with a voltage level of 1.04 p.u.

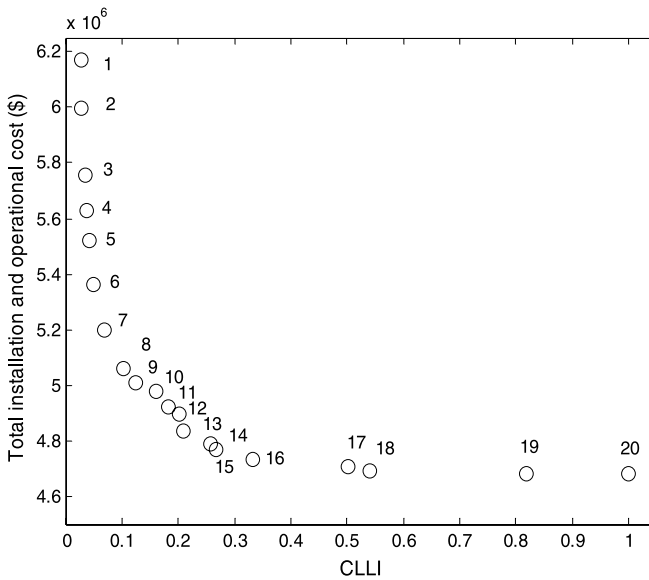


Fig. 24 Non-dominated solutions (of first stage planning) sampled for investigating the impacts of DG penetration

- *Case B*: The DG units are induction generators to which the reactive power is supplied by installation of local capacitor banks. The installation cost of capacitor banks is taken as \$3000/MVAr [40].
- *Case C*: The DG units are induction generators. They draw reactive power from the distribution supply system at power factors of 0.8.

The two objective functions for this planning are: total power loss and the DG penetration index as given in (3)–(4). The Pareto-approximation frontiers for all the three cases are shown in Fig. 25. The broken lines show the loci of the non-dominated solutions. The quantitative results are also given in Tables 8–10. They illustrate the following:

Remark 5 Some non-dominated solutions from the first stage planning become dominated after this planning stage. The radial networks with multiple feeders and meshed networks with longer loops mostly appear as the non-dominated solutions. It is observed that the DG units are mostly located in different feeders. The reason may be as follows: the inclusion of multiple DG units within a single feeder increases the node voltages to such high values that the upper voltage limit is violated. Thus, it helps to spread the sites of the DG units in different feeders. Among the three cases, the uniformly distributed non-dominated solutions are obtained in Case B. In Case A, no non-dominated solutions are obtained with the DG penetration indices between 0.41–0.93 and no non-dominated solutions are obtained beyond the DG penetration index of 0.23 in Case C.

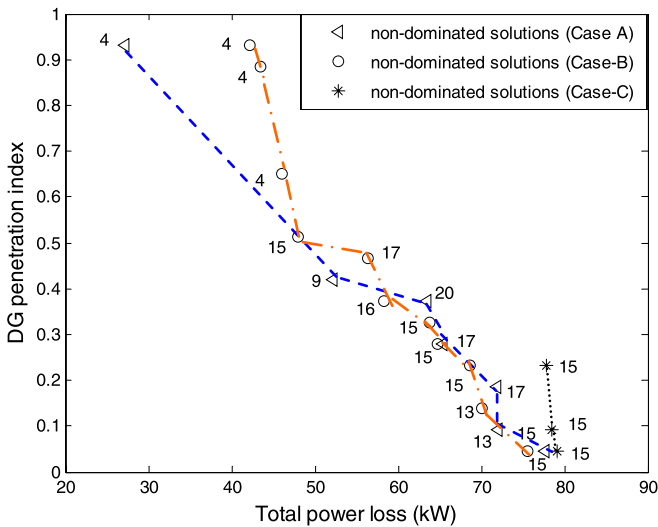


Fig. 25 Non-dominated solutions obtained from second stage of planning (after DG penetration)

Remark 6 Although the radial networks appear in the non-dominated solutions for Case A and Case B, they are not capable of DG penetration capacity of more than 50% of the total load (i.e., $\Psi > 0.5$). On the contrary, the meshed networks mostly appear in the non-dominated solutions when the DG penetration is higher. One possible reason may be that the radial networks experience over-voltage due to higher DG penetration. The results of Case A and Case B also indicate that, with the same DG penetration, the networks with synchronous generators have lower power loss as the synchronous generator can provide reactive power to the network resulting further reduction of power loss. Also the voltage profile with same DG penetration in Case B is slightly better because it is operated in the voltage controlled mode. In all the three cases, the minimum node voltage is significantly improved with DG penetration.

Remark 7 The DG penetration in Case C is restricted to 24% only as the generators draw reactive power at a constant power factor from the network. As the DG penetration increases, the generators consume more reactive power thereby increasing the power loss.

These results show that the cost of the network increases with higher DG penetration due to additional installation and operational cost, and the meshed networks can withstand more DG penetration than the radial networks.

4.3 Results of distribution system expansion planning

The proposed algorithm has also been applied to an expansion planning problem for the 21-node system [11]. This system has one substation at node-1 and some existing branches between the nodes 1–5. The nodes 6–21 are connected via the proposed

Table 8 Non-dominated solutions obtained from the second stage planning in Case A using the proposed MOPSO

Sol. No.	CLLI	DG Penetration index	Power loss (kW) after DG installation	Power loss (kW) before DG installation	Minimum voltage (p.u.) after DG installation	Minimum voltage (p.u.) before DG installation	Total network Cost with DG (\$)*10 ¹⁰	Configuration	N _{DG}	Sites of DG units (node number)	Size of DG units (kW)
15	0.2583	0.0466	77.6814	136.5686	1.0357	1.0271	0.0621	radial	1	11	500
13	0.2097	0.0931	71.9922	130.6776	1.0357	1.0277	0.1237	radial	2	15, 7	500, 500
17	0.5031	0.1863	71.8609	159.3054	1.0361	1.0262	0.2469	radial	1	56	2000
17	0.5031	0.2794	65.4837	159.3054	1.0392	1.0262	0.3701	radial	5	26, 17, 34, 6, 31	1000, 500, 500, 500, 500
20	1	0.3726	63.4483	207.9061	1.0379	1.0213	0.4932	radial	2	61, 6	2000, 2000
9	0.1030	0.4192	52.1954	290.853	1.041	1.0059	0.5549	mesh	3	98, 77, 99	500, 2000, 2000
4	0.0378	0.9315	27.1232	304.6879	1.0461	0.9973	1.2325	mesh	5	15, 81, 100, 35, 45	2000 each

Table 9 Non-dominated solutions after the second stage planning in Case B using the proposed MOPSO

Sol. No.	CLLI	DG Penetration index	Power loss (kW)		Minimum voltage (p.u.)		Total network Cost with DG (\$)*10 ¹⁰	Configuration	N _{DG}	Sites of DG units (node number)	Size of DG units (kW)
			after DG installation	before DG installation	after DG	before DG					
15	0.2583	0.0466	75.5498	136.5686	1.0357	1.0271	0.0622	radial	1	13	500
13	0.2097	0.1397	70.1069	130.6776	1.0357	1.0277	0.1856	radial	3	8, 31, 48	500 each
15	0.2583	0.2329	68.5792	136.5686	1.0357	1.0271	0.309	radial	5	32, 42, 37, 46, 52	500 each
15	0.2583	0.2794	64.7035	136.5686	1.0387	1.0271	0.3707	radial	3	99, 41, 92	500, 2000, 500
15	0.2583	0.326	63.771	136.5686	1.0357	1.0271	0.4324	radial	5	40, 3, 9, 28, 36	1000, 500, 1000, 500, 500
16	0.3332	0.3726	58.3546	158.7406	1.041	1.0266	0.4942	radial	2	51, 83	2000 each
17	0.5031	0.4657	56.3847	159.3054	1.0386	1.0262	0.6176	radial	4	5, 53, 65, 49	500, 2000, 2000, 500
15	0.2583	0.5123	48.0355	136.5686	1.0408	1.0271	0.6793	radial	5	29, 32, 31, 86, 51	500, 500, 1000, 2000, 1500
4	0.0378	0.652	46.0957	304.6879	1.041	0.9973	0.8645	mesh	5	13, 73, 41, 77, 50	500, 500, 2000, 2000, 2000
4	0.0378	0.8849	43.5448	304.6879	1.0413	0.9973	1.173	mesh	5	56, 5, 75, 98, 46	2000 each
4	0.0378	0.9315	42.2109	304.6879	1.0435	0.9973	1.2347	mesh	5	77, 39, 15, 42, 96	2000 each

Table 10 Non-dominated solutions obtained from the second stage planning in Case C using proposed MOPSO

Sol. No.	CLLI	DG Penetration index	Power loss (kW)		Minimum voltage (p.u.)		Total network Cost with DG (\$) [×] 10 ¹⁰	Configuration	N _{DG}	Sites of DG units (node number)	Size of DG units (kW)
			after DG installation	before DG installation	after DG	before DG					
15	0.2583	0.0466	79.189	136.5686	1.0357	1.0271	0.06209	radial	1	5	500
15	0.2583	0.0931	78.4933	136.5686	1.0357	1.0271	0.12369	radial	2	44, 33	500 each
15	0.2583	0.2329	77.7972	136.5686	1.0357	1.0271	0.30847	radial	5	17, 40, 50, 39, 25	500 each

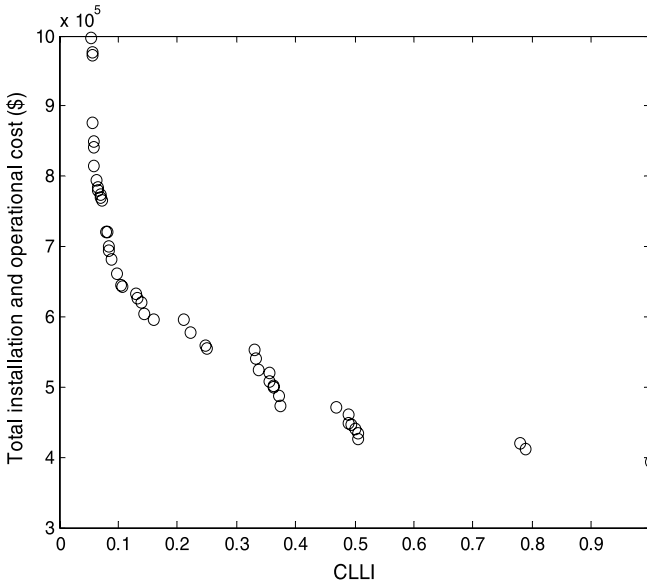
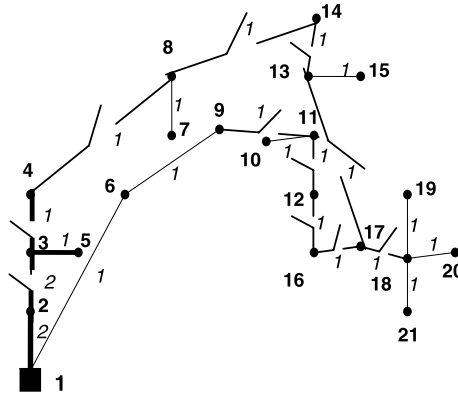


Fig. 26 Pareto-approximation frontier for the first stage expansion planning of the 21-node distribution system

Fig. 27 A typical solution network obtained with the expansion planning of 21-node distribution system



multi-objective planning algorithm. The specifications of the breaker and the conductor sizes used in this planning are the same as those given in the Tables 1–2. The maximum number of feeders, loops, and the allowable connections for a node are chosen as 5, 5, and 8, respectively. This planning is also done in two stages. The Pareto-approximation frontier obtained with the first stage planning is shown in Fig. 26. This frontier consists of a set of non-dominated solution networks with different number of loops, sectionalizing switches, and feeders. One sample solution network is also shown in Fig. 27 for illustration, where the existing branches are shown with bold lines. This network consists of 2 feeders, 9 sectionalizing switches, and one loop.

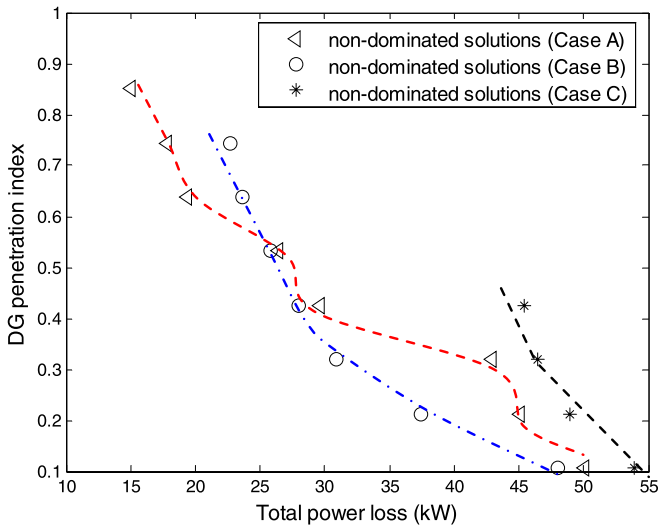


Fig. 28 Pareto-approximation frontiers for the second stage expansion planning of the 21-node distribution system

All solution networks are further evaluated in the second stage planning by optimizing the number, sites, and sizes of the DG units. The non-dominated solutions obtained with the second stage planning for the above mentioned three case studies (for the case of static planning) are given in Fig. 28. The approximate loci of the non-dominated solutions are shown as broken lines for better visualization. The results are similar to those reported for the static planning.

4.3.1 Sensitivity test with different number of strips per objective

The sensitivity test to assess the performance of the proposed MOPSO with different number of strips per objective is also carried out for the expansion planning of the 21-node distribution system. The results of this test for both the planning stages (considering Case B for Stage II) are given in Table 11. The reference points to determine the hypervolume indicator are taken as $(1.25 \times 10^6, 1)$ and $(1, 75)$ for Stage I and Stage II, respectively. The trend is almost similar to that obtained in the static planning problem. Hence, 15 strips per objective is a reasonably good choice and it has been used for both the planning stages in this study.

4.4 Performance comparison with an existing method

As the overall task including the objective function formulation in this work is different than those reported in the existing distribution system planning approaches, no direct performance comparison with those approaches is strictly possible. Hence, the proposed PSO-based algorithm is applied to optimize the objective functions formulated in [11] for expansion planning of the 21-node distribution system. The

Table 11 Hypervolume and diversity indicators with different number of strips per objective

Number of strips per each objective	Planning Stage I		Planning Stage II (Case B)	
	Mean hypervolume indicator	Mean diversity indicator	Mean hypervolume indicator	Mean diversity indicator
5	0.5581	0.7080	0.4385	0.1842
10	0.5608	0.6855	0.4757	0.1671
15	0.5659	0.6735	0.4921	0.1476
20	0.5672	0.6685	0.4921	0.1492
25	0.5691	0.6653	0.4893	0.1259

Table 12 Comparison of results between GA-based planning [11] and the proposed MOPSO-based planning

Solutions	Objective functions (GA [11]) (\$)		Objective functions (\$) (Proposed MOPSO)	
	First	Second	First	Second
	Most economical	6.7×10^5	843.79	6.59×10^5
Most reliable	17.07×10^5	7.71	10.01×10^5	12.8784

GA is used as the solution strategy in [11]. A quantitative performance comparison of the most reliable and the most economical solutions obtained from a Pareto-approximation frontier of the proposed MOPSO and the results reported in [11] are shown in Table 12. It shows that comparable results are obtained with the PSO-based approach. The advantages of the proposed planning algorithm are:

It is simpler to implement compared to the method used in [11]; there is no need for so many heuristic crossover and mutation operators as used in [11].

Each particle in the proposed MOPSO represents a connected network as the cost-biased encoding/decoding always creates connected network, unlike direct encoding.

Remark 8 It should be noted that this two-stage planning is non-iterative in the sense that the flow of the algorithm first completes the MOPSO for Stage I (for 200 iterations) and then, it is followed by the MOPSO for Stage II (for another 200 iterations). The schematic flow of this complete planning optimization process can be summarized as shown in Fig. 29(a). In this implementation, the output of the Stage II doesn't have any influence on the Stage I optimization. An alternative implementation of the flow of the optimization process is possible, where the feedback from the Stage II output can be used to influence the search. To incorporate the feedback from the Stage II output in a straightforward and simplistic manner, an iterative implementation of the Stage I and Stage II can be performed. In this iterative implementation of the optimization process, there is an overall optimization iteration and, in every iteration of the overall MOPSO, Stage I planning is performed followed by Stage II planning, where the output of the Stage II is fed back and used to influence the Stage I optimization. A schematic of this type of alternative implementation of the two-stage planning is summarized in Fig. 29(b). It can be foreseen that this approach will de-

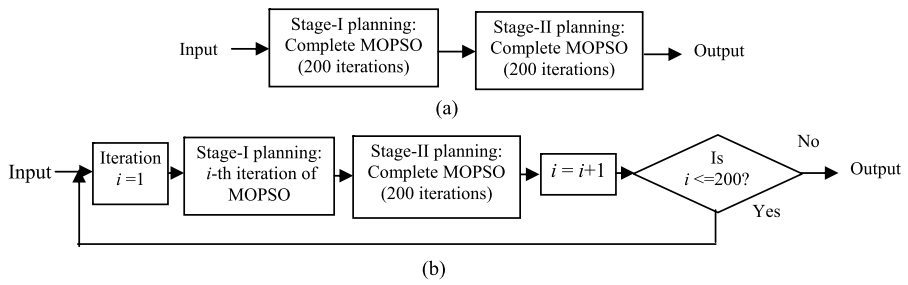


Fig. 29 (a) Non-iterative two-stage planning, and (b) Iterative two-stage planning

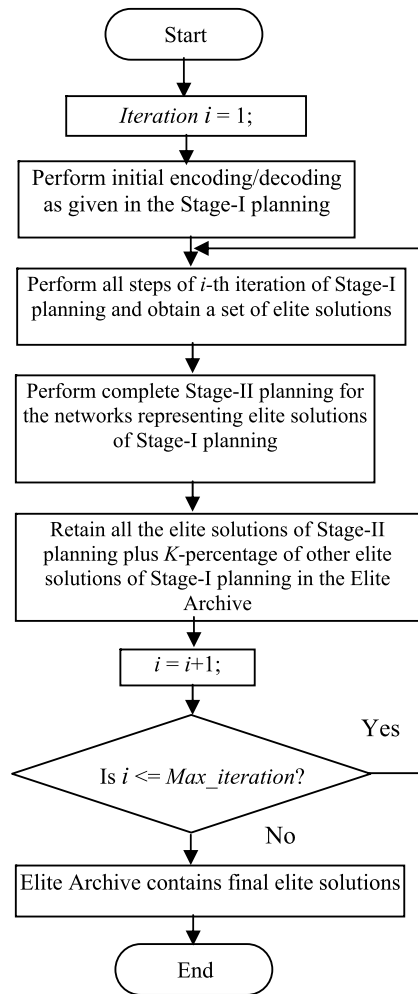
mand significant increase in computational time. Some simulation results for this iterative two-stage planning are given in the following subsection.

4.5 Iterative two-stage planning

As discussed in Remark 8, a simulation study is carried out to assess the relative performances of the iterative optimization of both planning stages. The detailed flow chart for the iterative two-stage planning is shown in Fig. 30. All the non-dominated/elite solutions obtained in the planning Stage I are processed in the Stage II. The elite solutions obtained after the planning Stage II represent the efficient networks for the DG integration. The elite archive, in an iteration, is designed to contain all the elite solutions obtained in the Stage II plus a certain pre-specified (K) percentage of the rest of the elite solutions from the Stage I. The intention is to guide the search in the Stage I considering the feedback from the Stage II. The K -percentage of the rest of the elite solutions from the Stage I are retained probabilistically in the elite archive in order to lessen the possibility of losing any potential solution that can play significant role in further search. This iterative optimization is tested for the 21-node system expansion planning.

The performance of this iterative optimization approach is compared with the previously used non-iterative two-stage optimization for two different values of K , i.e., 0% and 60%. The corresponding Pareto-approximation frontiers are shown in Fig. 31 considering Case B for the planning Stage II. The computational times (Processor: Intel Pentium D CPU 3 GHz 1 GB RAM) of a sample run with these two approaches are also given in Table 13. The results show that the performance of the iterative two-stage optimization is better than that of the non-iterative two-stage planning with $K = 60$ (and worse with $K = 0$). This illustrates that the iterative optimization mostly performs better when some of the elite solutions of Stage I are kept in the elite archive. The reason is due to the provision of retaining some potential guiding solutions from Stage I in the elite archive with a nonzero K . Thus, a better performance can be expected in the iterative approach with proper management of the elite archive. However, it should be noted that the computational time requirement also increases dramatically compared to the non-iterative two-stage planning. It is almost 25 times higher than that of the non-iterative planning for this comparatively smaller

Fig. 30 Flow chart for the iterative two-stage planning



21-node system. This is expected because one complete Stage II planning optimization is required in every iteration and the computational demand will be extremely high for higher node systems. This happens to be a significant limitation of the iterative planning.

In addition to higher computational burden, there is one more issue associated with the iterative two-stage planning. As mentioned earlier, the DG integration is not always possible for all the utilities and areas. In these circumstances, the first stage planning is only required. Thus, it is worth comparing the quality of the solutions obtained after the planning Stage I with the non-iterative and iterative approaches. The Pareto-approximation frontiers based on the objective functions used in the planning Stage I, obtained with the iterative and non-iterative two-stage planning, are shown in Fig. 32. It illustrates that the non-dominated solutions obtained with the iterative two-stage planning are restricted within a certain area (shown as a dotted enclosure) of the objective space caused by the search for the networks efficient for DG integration.

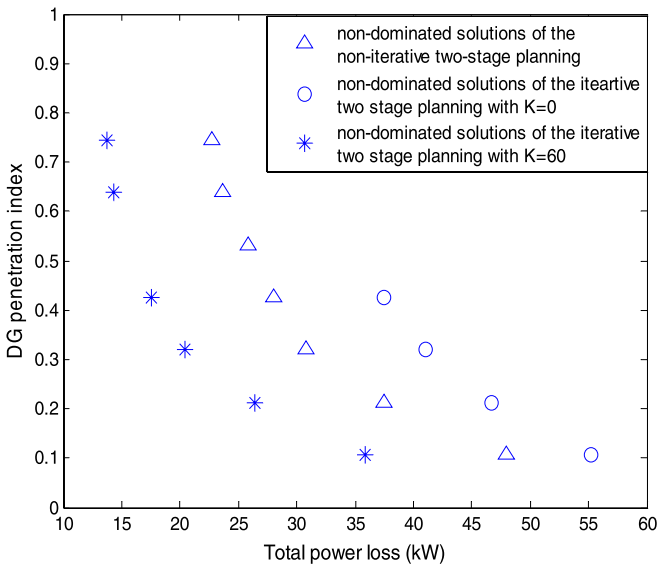


Fig. 31 Comparison of the Pareto-approximation frontiers for the 21-node system obtained with the non-iterative two-stage planning and the iterative two-stage planning

Table 13 Comparison of computational time requirement and hypervolume indicator of the Pareto-approximation frontiers between the non-iterative two-stage planning and the iterative two-stage planning for the 21-node system

Planning optimization approaches	Computational time per run (min)	Hypervolume indicator (ref point = (50, 1))
Non-iterative two-stage planning	16.2	0.3656
Iterative two-stage planning ($K = 60\%$)	418.2	0.5425

Hence, if the DG integration is not desired, the utility will definitely get a better solution set from the planning Stage I with the non-iterative two-stage planning approach compared to the other.

5 Conclusion

In this paper, a novel multi-objective PSO-based planning of the power distribution systems incorporating distributed generation (DG) has been investigated. This planning consists of two stages, i.e., Stage I and Stage II. In Stage I, a multi-objective planning of the power distribution systems without DG is done. The two objectives of the first stage planning optimization are: (i) total installation and operational cost and (ii) the contingency-load-loss index (CLLI). The CLLI is computed by considering contingencies in all the network branches, taken one at a time. A tradeoff analysis of these two conflicting objectives is done by using the Pareto-optimality principle to

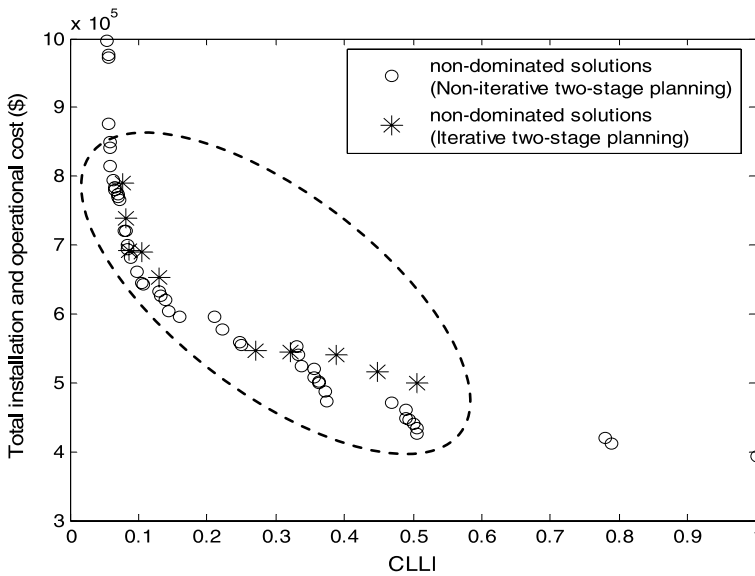


Fig. 32 Comparison of the Pareto-approximation frontiers based on the two objective functions of the planning Stage I for the 21-node system obtained with the non-iterative and iterative two-stage planning

obtain a set of non-dominated solutions; each solution represents a network structure (radial/meshed), branch conductor sizes, and the number and locations of the sectionalizing switches. A novel multi-objective PSO (MOPSO) has been proposed for an efficient leader selection mechanism so as to have an effective search. A set of leaders consisting of the non-dominated solutions and some selected dominated solutions is chosen to guide the search in the proposed method. To choose the dominated solutions for potential leaders, the objective space is divided into a number strips per objective. A dominated solution is considered as a leader from a strip if no non-dominated solution is available in that strip. A novel cost-biased encoding/decoding scheme is devised for the representation of the particles in the MOPSO for preventing the creation of infeasible networks. Further, additional mechanisms have been incorporated for creation of meshed networks and placement of the sectionalizing switches. The performance of the algorithm is assessed and compared with that of the well-established SPEA2-based PSO and some existing MOPSO algorithms by several statistical tests. The tests show that the performance of the proposed MOPSO is better compared to those of the SPEA2-based PSO and other MOPSO algorithms. In the second stage planning, the impact of the DG on different network structures (obtained from the non-dominated solutions of the first stage planning) has been investigated for both radial and meshed networks. The proposed MOPSO has been tested for both static and expansion planning on typical 100-node and 21-node distribution systems, respectively. Sensitivity tests are carried to obtain the optimal number of strips per objective and the order of penalty factors (for the cases of constraint violations) used in this planning.

The significant contributions in this paper are: development of a novel and effective leader selection mechanism for the MOPSO, a novel particle encoding/decoding

scheme for the planning of distribution networks that when decoded can create radial/meshed networks with single/multiple feeders and sectionalizing switches, and incorporation of the DG in the network planning via multi-objective optimization. However, it is worth mentioning that this planning algorithm can be further extended for multi-stage planning to handle future load growth more efficiently.

A planning approach combining all the four objectives used in this two-stage optimization in a more general framework for an overall single-stage optimization is another important area for future research. Such an advanced planning approach may prove to be beneficial for those utilities/areas where the DG can be surely integrated and it is a promising area for future work.

Appendix

This appendix provides some basics of the short circuit capacity calculation used to select the substation circuit breaker's rating, the SPEA2-based PSO, Mann-Whitney rank sum test, and the load demand data of the 21-node and 100-node distribution systems.

A.1 Short circuit capacity calculation for distribution networks

The short circuit capacity calculation is required for this study because the radial and meshed networks have different short circuit capacities. The short circuit capacity of a meshed network is higher than that of a radial network. Hence, it is very much essential to select the circuit breakers and the protection system accordingly. In this work, the maximum short circuit capacity of a distribution network is calculated by the short circuit MVA calculation method [39]. The maximum short circuit current is possible if the fault occurs at a location closer to the substation main bus; thus the short circuit capacity is higher at the substation and it gradually reduces if the fault point shifts away from the substation. The short circuit MVA capacity of the different components of a distribution network can be obtained as:

The short circuit MVA of a substation transformer of S_{rated} MVA and impedance of Z_{pu} p.u. is:

$$MVA_{SC}^{Tr} = S_{rated} / Z_{pu} \quad (A.1)$$

The short circuit MVA of a feeder branch with voltage level of kV and impedance of Z_{Ω} ohm is:

$$MVA_{SC}^{Br} = (kV)^2 / Z_{\Omega} \quad (A.2)$$

The aggregated short circuit capacity of H components can be obtained as follows:

If the components are connected in series:

$$MVA_{SC}^{Series} = \sum_{i=1}^H (1/MVA_{SCi}) \quad (A.3)$$

If the components are connected in parallel:

$$MVA_{SC}^{Parallel} = \sum_{i=1}^H MVA_{SC_i} \quad (A.4)$$

In this work, the short circuit capacity of a network is calculated by considering a fault at the substation bus using (A.1)–(A.4). The net short circuit current is derived from the resultant short circuit MVA of the network as:

$$I_{SC} = MVA_{SC}/KV \quad (A.5)$$

With DG, the net short circuit current is calculated as:

$$I_{SC}^{DG} = I_{SC} + \sum_{i=1}^{N_{DG}} I_i^{DG} \quad (A.6)$$

(I_i^{DG} : short circuit current contribution of the i -th DG).

A.2 SPEA2-based PSO

The SPEA2 is a multi-objective optimization algorithm [36], where an elite archive is created to preserve the non-dominated solutions found by the algorithm and this elite archive is used to assign fitness to each member of the archive itself and the current population undergoing evolution to assist the search for more non-dominated solutions. Thus, the SPEA2 handles two populations of solutions, i.e., elite archive (say E) and PSO population of current iteration (F). The sequential steps for the fitness assignment are:

- Certain *strength* (proportional to the number of dominated members/solutions) is assigned to all current and elite members. The strength of a member i , $\delta(i)$, is defined as:

$$\delta(i) = \{j | j \in (E + F) \wedge i < j\} \quad (A.7)$$

- Then, a *raw fitness* equal to the sum of the strengths of the dominators of the concerned member is assigned to each current and elite member. The raw fitness $\xi_R(i)$ of member i of is the sum of its dominator's strength given by:

$$\xi_R(i) = \sum_{j \in (A+B) \wedge i > j} \delta(j) \quad (A.8)$$

- Finally, the *fitness* of a member (current/elite) is computed as the summation of its raw fitness and density around it. The density of a member i , $\zeta(i)$, is defined as the inverse of the distance of its k -th nearest data point. The value of k is the square root of sum of population and archive size. The fitness of the member i , $\gamma(i)$, is computed as:

$$\gamma(i) = \xi_R(i) + \zeta(i) \quad (A.9)$$

Begin

Initialize $E = F = \emptyset$;

Set maximum iteration (Max_iter), population size (Pop_size), and elite archive size ($elite_size$);

For $i = 1, \dots, Max_iter$

Update position and velocity of all particles using their respective $pbest$ and the $gbest$;

Calculate the objective functions;

Find out the non-dominated solutions from F and transferred them into E ;

Extract the resultant non-dominated solutions and update E ;

Assign fitness to all members of E and F using (A.7)–(A.9);

If $size\{E\} > elite_size$

Calculate the Euclidean distances (τ) among all adjacent solutions and sort them in ascending order;

Remove ($size\{E\} - elite_size$) number of solutions from E having lower τ ;

Elseif $size\{E\} < elite_size$

Insert ($elite_size - size\{E\}$) number of dominated solutions into E having better fitness;

Endif

Identify the group best particle based on fitness and store its position at $gbest$;

Endfor

The elite archive contains the final non-dominated solutions.

End

Fig. A.1 Pseudocodes of the SPEA2-based PSO

The strategy is to assign lower fitness to the preferred solutions (as this is a minimization problem). The raw fitness of a non-dominated solution is zero as it doesn't have a dominator. The solutions in the dense areas are penalized with their densities. This fitness assignment helps to orient the search towards unexplored regions of the non-dominated solutions. The pseudocodes for the SPEA2 based PSO are given in Fig. A.1.

A.3 Calculation of the U statistic in the Mann-Whitney rank sum test

Let $d_1(d_2)$ be the sum of the ranks given to the observations in group 1 (group 2) and $g_1(g_2)$ be the total number of observations in group 1 (group 2). A statistic U_1 is assigned to the group 1 as:

$$U_1 = d_1 - g_1(g_1 + 1)/2 \quad (\text{A.10})$$

Similarly, a statistic U_2 is assigned to the group 2. The null hypothesis can be rejected if:

$$\min(U_1, U_2) \leq U_{critical} \quad (\text{A.11})$$

A.4 Data of 21-node distribution system

Table A.1 Node location and load demand for the 21-node distribution system

<i>N</i>	<i>X</i>	<i>Y</i>	<i>L_{RL}</i>	<i>L_{RV}</i>	<i>N</i>	<i>X</i>	<i>Y</i>	<i>L_{RL}</i>	<i>L_{RV}</i>	<i>N</i>	<i>X</i>	<i>Y</i>	<i>L_{RL}</i>	<i>L_{RV}</i>
1	1	1	0	0	8	6	4	100	20	15	6	8	100	50
2	2	1	200	50	9	5.1	5	200	100	16	3	7	400	100
3	3	1	100	20	10	4.9	6	500	200	17	3.1	8	750	90
4	4	1	150	60	11	5	7	900	200	18	2.9	9	100	40
5	5	2	200	50	12	4	7	100	20	19	4	9	100	40
6	4	3	250	80	13	6	6.9	100	20	20	3	10	100	40
7	5	4	50	5	14	7	7	200	50	21	2	9	100	40

Notes: *N* = index of node, *X* (*Y*): locations of nodes (km); Substation voltage = 1.05 p.u. Base voltage = 13.8 kV; *L_{RL}*: Real power demand in kW; *L_{RV}*: Reactive power demand in kVAr

A.5 Data of 100-node distribution system

Table A.2 Node location and load demand for the 100-node distribution system

<i>N</i>	<i>X</i>	<i>Y</i>	<i>L</i>	<i>N</i>	<i>X</i>	<i>Y</i>	<i>L</i>	<i>N</i>	<i>X</i>	<i>Y</i>	<i>L</i>	<i>N</i>	<i>X</i>	<i>Y</i>	<i>L</i>
1	10	3.5	0	26	4	4	140	51	5	8	120	76	4	13	145
2	1	0	125	27	10	4	110	52	17	8	210	77	6	13	110
3	7	0	110	28	12	4	110	53	19	8	130	78	8	13	115
4	8	0	130	29	14	4	100	54	0	9	210	79	12	13	100
5	10	0	150	30	16	4	100	55	1	9	130	80	14	13	130
6	11	0	140	31	18	4	100	56	2	9	110	81	1	14	130
7	13	0	110	32	1	5	135	57	4	9	115	82	4	14	125
8	15	0	115	33	5	5	200	58	8	9	125	83	6	14	100
9	16	0	90	34	7	5	160	59	9	9	130	84	8	14	140
10	1	1	200	35	9	5	110	60	11	10	190	85	15	14	150
11	2	1	75	36	14	5	120	61	13	10	170	86	4	15	140
12	4	1	160	37	0	6	100	62	18	10	100	87	7	15	140
13	5	1	120	38	2	6	130	63	2	11	120	88	12	15	125
14	6	1	130	39	4	6	130	64	4	11	130	89	14	15	115
15	9	1	140	40	7	6	190	65	6	11	130	90	1	16	180
16	12	1	110	41	11	6	100	66	8	11	125	91	2	16	120
17	13	2	100	42	13	6	130	67	10	11	110	92	3	17	110
18	15	2	120	43	16	6	140	68	15	11	125	93	4	17	100
19	0	3	110	44	17	6	110	69	17	11	90	94	7	17	130
20	2	3	185	45	19	6	115	70	18	11	180	95	8	17	150
21	5	3	140	46	6	7	120	71	0	12	110	96	11	17	120

Table A.2 (Continued)

<i>N</i>	<i>X</i>	<i>Y</i>	<i>L</i>	<i>N</i>	<i>X</i>	<i>Y</i>	<i>L</i>	<i>N</i>	<i>X</i>	<i>Y</i>	<i>L</i>	<i>N</i>	<i>X</i>	<i>Y</i>	<i>L</i>
22	7	3	75	47	9	7	175	72	1	12	130	97	13	17	120
23	9	3	150	48	15	7	100	73	7	12	100	98	8	18	125
24	14	3	120	49	0	8	100	74	11	12	130	99	9	18	100
25	2	4	130	50	4	8	90	75	13	12	140	100	11	18	100

Notes: *N* = index of node; *X* = *X*-coordinate of node (Km); *Y* = *Y*-coordinate of node (Km); *L* = Load demand (KVA)

Other data: Power factor = 0.85; Substation voltage = 1.05 p.u.; Base voltage = 34.8 kV; Energy cost = \$60/MWh

References

- Gonen, T., Ramirez-Rosado, I.J.: Review of distribution system planning models: a model for optimal multi-stage planning. *IEE Proc. C* **133**(7), 397–408 (1986)
- Khator, S.K., Leung, L.C.: Power distribution planning: a review of models and issues. *IEEE Trans. Power Syst.* **12**(3), 1151–1159 (1997)
- Fletcher, R.H., Strunz, K.: Optimal distribution system horizon planning—Part I: formulation. *IEEE Trans. Power Syst.* **22**(2), 791–799 (2007)
- Fletcher, R.H., Strunz, K.: Optimal distribution system horizon planning—Part II: application. *IEEE Trans. Power Syst.* **22**(2), 862–870 (2007)
- Nahman, J., Spiric, J.: Optimal planning of rural medium voltage distribution networks. *Electr. Power Energy Syst.* **19**(8), 549–556 (1997)
- Boulaxis, N.G., Papadopoulos, M.P.: Optimal feeder routing in distribution system planning using dynamic programming technique and GIS facilities. *IEEE Trans. Power Deliv.* **17**(1), 242–247 (2002)
- Miranda, V., Ranito, J.V., Proenca, L.M.: Genetic algorithm in optimal multistage distribution network planning. *IEEE Trans. Power Syst.* **9**(4), 1927–1931 (1994)
- Tang, Y.: Power distribution systems planning with reliability modeling and optimization. *IEEE Trans. Power Syst.* **11**(1), 181–189 (1995)
- Kagan, N., Adams, R.N.: A Benders' decomposition approach to the multi-objective distribution planning problem. *Int. J. Electr. Power Energy Syst.* **15**(5), 259–271 (1993)
- Ramirez-Rosado, I.J., Bernal-Agustín, J.L.: Reliability and costs optimization for distribution networks expansion using an evolutionary algorithm. *IEEE Trans. Power Syst.* **16**(1), 111–118 (2001)
- Carrano, E.G., Soares, L.A.E., Takahashi, R.H.C., Saldanha, R.R., Neto, O.M.: Electric distribution network multiobjective design using a problem-specific genetic algorithm. *IEEE Trans. Power Deliv.* **21**(2), 995–1005 (2006)
- Mendoza, F., Agustín, J.B., Dominguez-Navarro, J.A.: NSGA and SPEA applied to multiobjective design of power distribution systems. *IEEE Trans. Power Syst.* **21**(4), 1938–1945 (2006)
- Rivas-Dávalos, F., Irving, M.R.: An approach based on the strength Pareto evolutionary algorithm 2 for power distribution system planning. In: *Lecture Notes in Computer Science*, vol. 3410, pp. 707–720. Springer, Berlin (2005)
- Ramirez-Rosado, I.J., Dominguez-Navarro, J.A.: New multi-objective Tabu Search algorithm for fuzzy optimal planning of power distribution systems. *IEEE Trans. Power Syst.* **21**(1), 224–233 (2006)
- Carrano, E.G., Guimaraes, F.G., Takahashi, R.H.C., Neto, O.M., Campelo, F.: Electric distribution network expansion under load-evolution uncertainty using an immune system inspired algorithm. *IEEE Trans. Power Syst.* **22**(2), 851–861 (2007)
- Billinton, R., Allan, R.N.: *Reliability Evaluation of Power Systems*, 2nd edn. Springer, Berlin (1992)
- Celli, G., Pilo, F., Pisano, G., Allegranza, V., Cicoria, R., Iaria, A.: Meshed vs. radial MV distribution network in presence of large amount of DG. In: *IEEE PES Power Systems Conference and Exposition* vol. 2, pp. 709–714 (2004)
- Celli, G., Ghiani, E., Loddo, M., Pilo, F.: An heuristic technique for the optimal planning of meshed MV distribution network. In: *IEEE Russia Power Tech.*, pp. 1–7 (2008)

19. Pecas Lopes, J.A., Hatziaargyriou, N., Mutale, J., Djapic, P., Jenkins, N.: Integrating distributed generation into electric power systems: a review of drivers, challenges and opportunities. *Electr. Power Syst. Res.* **77**, 1189–1203 (2007)
20. El-Khattam, W., Salama, M.M.A.: Distribution system planning using distributed generation. In: *Canadian Conference on Electrical and Computer Engineering. Toward a Caring and Humane Technology*, vol. 1, pp. 579–582 (2003)
21. Chiradeja, P., Ramakumar, R.: An approach to quantify the technical benefits of distributed generation. *IEEE Trans. Energy Convers.* **19**(4), 764–773 (2004)
22. Ochoa, L.F., Feltrin, A.P., Harrison, G.P.: Evaluating distributed generation impacts with a multiobjective index. *IEEE Trans. Power Deliv.* **21**(3), 1452–1458 (2006)
23. Celli, G., Ghiani, E., Mocci, S., Pilo, F.: A multiobjective evolutionary algorithm for the sizing and siting of distributed generation. *IEEE Trans. Power Syst.* **20**(2), 750–757 (2005)
24. Carpinelli, G., Celli, G., Mocci, S., Pilo, F., Russo, A.: Optimisation of embedded generation sizing and siting by using a double trade-off method. *IEE Proc. Gener. Transm. Distrib.* **152**(4), 503–513 (2005)
25. Haffner, S., Pereira, L.F.A., Pereira, L.A., Barreto, L.S.: Multistage model for distribution expansion planning with distributed generation—part I: problem formulation. *IEEE Trans. Power Deliv.* **23**(2), 915–923 (2008)
26. Haffner, S., Pereira, L.F.A., Pereira, L.A., Barreto, L.S.: Multistage model for distribution expansion planning with distributed generation—part II: numerical analysis. *IEEE Trans. Power Deliv.* **23**(2), 924–929 (2008)
27. Singh, D., Misra, R.K., Singh, D.: Effect of load models in distributed generation planning. *IEEE Trans. Power Syst.* **22**(4), 2204–2212 (2007)
28. Singh, D., Singh, D., Verma, K.S.: Multiobjective optimization for DG planning with load models. *IEEE Trans. Power Syst.* **24**(1), 427–436 (2009)
29. Mantway, A.H., Al-Muhaini, M.M.: Multi-objective BPSO algorithm for distribution system expansion planning including distributed generation. In: *IEEE/PES Transmission and Distribution Conference and Exposition*, pp. 1–8 (2008)
30. De-Souza, B.A., De-Albuquerque, J.M.C.: Optimal placement of distributed generators networks using evolutionary programming. In: *IEEE/PES Transmission & Distribution Conference & Exposition: Latin America*, p. 6 (2006)
31. Deb, K.: *Multi-Objective Optimization using Evolutionary Algorithms*. Wiley, New York (2004)
32. Kennedy, J., Eberhart, R.C.: Particle swarm optimization. In: *Proc. of IEEE International Conference on Neural Networks*, Perth, Australia, pp. 1942–1948 (1995)
33. Shi, Y., Eberhart, R.C.: A modified particle swarm optimizer. In: *Proc. IEEE Congress of Evolutionary Computation*, pp. 69–73 (1998)
34. Valle, Y., Venayagamoorthy, G.K., Mohagheghi, S., Hernandez, J., Harley, R.G.: Particle swarm optimization: basic concepts, variants and applications in power systems. *IEEE Trans. Evol. Comput.* **12**(2), 171–195 (2008)
35. Sierra, M.R., Coello Coello, C.A.: Multi-objective particle swarm optimizers: a survey of the state-of-the-art. *Int. J. Comput. Intell. Res.* **2**(3), 287–308 (2006)
36. Zitzler, E., Laumanns, M., Thiele, L.: SPEA2: improving the strength Pareto evolutionary algorithm. *Computer Engineering and Networks Laboratory Technical Report-103*, ETH, Zurich, Switzerland (2001)
37. Mohemmed, A.W., Sahoo, N.C.: Particle swarm optimization combined with local search and velocity re-initialization for shortest path computation in networks. In: *Proc. of IEEE Swarm Intelligence Symposium*, pp. 266–272 (2007)
38. Knowles, J.D., Thiele, L., Zitzler, E.: A tutorial of the performance assessment of stochastic multi-objective optimizers. *Computer Engineering and Networks Laboratory Technical Report-214*, ETH, Zurich, Switzerland (2006)
39. Chen, T.H., Huang, W.T.: Evaluation of the variations of short-circuit capacities along a feeder due to distribution system-type upgrading. *Electr. Power Energy Syst.* **31**, 50–58 (2009)
40. Das, D.: Optimal placement of capacitors in radial distribution system using a Fuzzy-GA method. *Electr. Power Energy Syst.* **30**, 361–367 (2008)
41. Sahoo, N.C., Ganguly, S., Das, D.: A two-step contingency-based multi-objective planning of electrical distribution systems using particle swarm optimization. *J. Electr. Eng.* (submitted)
42. Parsopoulos, K.E., Vrahatis, M.N.: Multiobjective particle swarm optimization approaches. In: *Multi-Objective Optimization in Computational Intelligence: Theory and Practice*, pp. 20–42. IGI Global, Hershey (2008), Chap. 2

43. Durillo, J.J., García-Nieto, J., Nebro, A.J., Coello Coello, C.A., Luna, F., Alba, E.: Multi-objective particle swarm optimizers: an experimental comparison. In: *Lecture Notes in Computer Science*, vol. 5467, pp. 495–509. Springer, Berlin (2009)
44. Wickramasinghe, W., Li, X.: Integrating user preferences with particle swarms for multi-objective optimization. In: *GECCO'08*, Atlanta, USA, pp. 745–752 (2008)
45. Miranda, V., Keko, H., Duque, A.J.: Stochastic star communication topology in evolutionary particle swarms (EPSO). *Int. J. Comput. Intell. Res.* **4**(2), 105–116 (2008)
46. Nebro, A.J., Durillo, J.J., Luna, F., Dorronsoro, B., Alba, E.: Design issues in a multiobjective cellular genetic algorithm. In: *Lecture Notes in Computer Science*, vol. 4403, pp. 126–140 Springer, Berlin (2007)
47. Qin, Y., Wang, J.: Distribution network reconfiguration based on particle clonal genetic algorithm. *J. Comput.* **4**(9), 813–820 (2009)
48. Kuri-Morales, A.F., Gutiérrez-García, J.: Penalty function methods for constrained optimization with genetic algorithms: a statistical analysis. In: *Lecture Notes in Computer Science*, vol. 2313, pp. 108–117. Springer, Berlin (2002)